Copolymer/Clay Nanocomposites for Biomedical Applications

Selvakumar Murugesan and Thomas Scheibel

Nanoclays still hold a great strength in biomedical nanotechnology applications due to their exceptional properties despite the development of several new nanostructured materials. This article reviews the recent advances in copolymer/clay nanocomposites with a focus on health care applications. In general, the structure of clay comprises aluminosilicate layers separated by a few nanometers. Recently, nanoclay-incorporated copolymers have attracted the interest of both researchers and industry due to their phenomenal properties such as barrier function, stiffness, thermal/flame resistance, superhydrophobicity, biocompatibility, stimuli responsiveness, sustained drug release, resistance to hydrolysis, outstanding dynamic mechanical properties including resilience and low temperature flexibility, excellent hydrolytic stability, and antimicrobial properties. Surface modification of nanoclays provides additional properties due to improved adhesion between the polymer matrix and the nanoclay, high surface free energy, a high degree of intercalation, or exfoliated morphology. The architecture of the copolymer/clay nanocomposites has great impact on biomedical applications, too, by providing various cues especially in drug delivery systems and regenerative medicine.

1. Introduction

Nanocomposites can be defined as a class of new materials with a dispersed phase (fillers) having at least one of its dimensions in the nanometer regime. Nanocomposites have been commonly used in rubber or polymer technology providing silica (SiO_2) and carbon black as a reinforcing filler, especially in the tire industry, without terming it as nanotechnology. As compared to traditional composites (macro or micro scale fillers), nanocomposites possess various exceptional qualities as well as properties at a very low level of filler reinforcement due to their unique physical characteristics of nanostructured materials such as increased surface area, architecture and functionalities, surface energy, and high strength-to-weight ratio.[1]

Copolymers used as matrix in nanocomposites, contain at least two segments with different properties and characteristics. As a result, a microphase partition can occur. Various catalysts, initiators and chain extenders have been used for the synthesis of different types of copolymers in order to change the properties as well as obtaining accustomed morphologies. Such changes significantly influence the physico-mechanical properties and other functional characteristics of the respective copolymers.

Nanoclays are minerals with varying chemical composition and possess unique architectures with varying morphologies. Nanoclays are layered aluminosilicates divided by interlayers with only a few nanometers. In nanotechnological terms, nanoclays have been classified as 2D nanomaterials.[2]

The first report on polymer-based nanocomposites can be found back in the early 1960s on methyl methacrylate-based polymer chains adsorbed on the surface of montmorillonite (MMT) clay by Prof. A. Blumstein.[3] Thereafter, studies were conducted on amalgamation of clays in various types of polymeric matrix such as thermoplastics,[4] thermosets[5] and elastomers.[6] The first successful attempt to produce nylon-6/silicate clay nanocomposites from the research group of Toyota[7] has been the motivation for the development of fabricating advanced polymeric/nanoclay composites, for example, aircraft and biomedical applications. So far, most of the known nanoclay minerals such as MMT, bentonite, sepiolite, laponite, and layered double hydroxide (LDH), a synthetic type of clay, have been implemented in a polymer matrix for fabricating nanocomposites for different applications.[8] The aforementioned different clays are derived from either solid rocks or they are synthesized. Among those clays, MMT clay has been used in both laboratory research as well as in industry for manufacturing commercial products due to cost effectiveness as well as good compatibility with most polymers.[4a,d,9] In the first report on the preparation of polyurethane-based copolymer/clay nanocomposites by Wang and Pinnavaia,[10] they exhibited excellent mechanical strength without compromising optical transparency. One can obtain a wide range of properties by just tuning the phase morphology or chemical architecture of copolymer/clay nanocomposites. Owing to their physical and mechanical characteristics, they have been used as shape memory materials, drug carrier, membranes, nanovehicles, biodegradable bio-implants, scaffolds, coatings,

Dr. S. Murugesan, Prof. T. Scheibel
Lehrstuhl Biomaterialien
Universität Bayreuth
Prof.-Rüdiger-Bormann-Str. 1, 95447 Bayreuth, Germany
E-mail: thomas.scheibel@bm.uni-bayreuth.de
Prof. T. Scheibel
Bayreuther Zentrum für Kolloide und Grenzflächen (BZKG)
Bayreuther Zentrum für Molekulare Biowissenschaften (BZMB)
Bayreuther Materialzentrum (BayMAT)
Bayerisches Polymerinstitut (BPI)
University Bayreuth
Universitätsstr. 30, 95447 Bayreuth, Germany

The ORCID identification number(s) for the author(s) of this article can be found under https://doi.org/10.1002/adfm.201908101.

**ADVANCED
SCIENCE NEWS**
www.advancedsciencenews.com

**ADVANCED
FUNCTIONAL
MATERIALS**
www.afm-journal.de

foams, and fibers,[11] in order to improve, for example, biocompatibility or barrier properties, which are difficult to achieve by adding other nanofillers.[12] Clay reinforcements of copolymers can enrich various further characteristics such as antimicrobial properties, shape recovery, conductivity (electrical and thermal), targeted delivery of biomolecules or drugs, compatibility with blood and living tissue/organs and biodegradability.[13]

The basic route of preparation of copolymer/clay nanocomposites is either placing the polymer chains in-between or to polymerize the desired monomers/precursors in-between clay layers.[15] The dispersion morphology of clay incorporated into copolymers is divided into three types, namely i) intercalation, ii) flocculation, and iii) exfoliation. These three dispersion morphologies are displayed schematically in **Figure 1**. The Toyota research group reported an intercalated polymer composite morphology with macromolecule chains inserted into silicate layer galleries with a few nanometer distances between the basal planes (d_{001}) of the crystal. In a flocculation morphology, polymer chains were intercalated, and subsequently the clay layers stacked one on another to certain distance because of their edge–edge interactions, especially based on hydroxyl group (–OH) interactions. Upon exfoliation, complete or partial delamination of individual layers of clay in the polymer matrix took place, which resulted from an extensive diffusion of the polymer chains into the interlayer d-spacing (001). The average distance of delaminated layers depended upon many factors such as the amount of clay loading in a copolymer matrix, clay functionalities, as well as interfacial interaction between matrix and clay. However, the clay platelets would not maintain uniform layer spacing's since no sufficient attractions exist between the silicate layers.[14] It has been proposed that the physico-mechanical properties of exfoliated copolymer/clay morphologies are more dominant than that of intercalated ones.[9a,16] However, the complete exfoliation of nanoclays is fairly difficult to accomplish as repulsion forces exist between clay and polymer matrix. Therefore, surface modification of clays is important for improving the compatibility with hydrophobic copolymers, since clays are often hydrophilic.[17] Concerning biomedical applications,[18] the increment in the gallery space of nanoclays is highly beneficial, especially in drug delivery materials.[13] More space between the clay layers allows for a higher loading efficiency.

Polymer/clay nanocomposites including their 3D bioprinting have been reviewed recently for different biomedical applications.[19] Gaharwar et al.[20] reviewed the potential of laponite nanoclay and its nanocomposites for additive manufacturing

Selvakumar Murugesan received his bachelor's degree in polymer technology from Anna University, Chennai (India) in 2009 and master's degree in materials engineering from National Institute of Technology, Karnataka (India) in 2011. Then, he earned his doctoral degree from Indian Institute of Technology Kharagpur in the area of polymer hybrids for biomedical applications (2016). He is currently a postdoctoral student in Thomas Scheibel's group; emphasis of his research is on development of novel biomaterials based on recombinant spider silk proteins for tissue engineering applications.

Thomas Scheibel has been full professor at the department of biomaterials at the Universität Bayreuth in Germany since 2007. He received both his diploma of biochemistry (1994) and a Dr. rer. nat. (1998) from the Universität Regensburg in Germany. After his postdoctoral stay at the University of Chicago (1998–2001), he received his habilitation (2007) from the Technische Universität München in Germany. His research focuses on biotechnological production and processing of structural proteins, as well as their biomedical and technical application.

and regenerative medicine. Liu et al.[21] reported an overview of halloysite nanotubes and respective nanocomposites for various biomedical applications such as drug delivery, biosensing, and bone regeneration. Chimene et al.[22] extensively reviewed nanoclay reinforced hydrogels as bioinks for 3D bioprinting.

In our present article a broad overview is provided over several classes of nanoclays, copolymers various modification protocols, and processing methodologies to prepare different
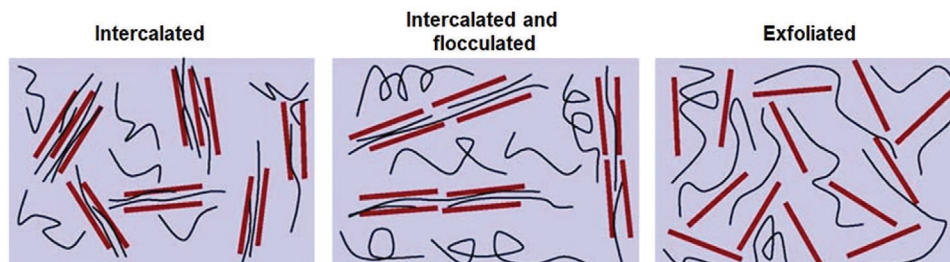
Figure 1. Illustration of the morphology of clay dispersion in a polymer matrix. Reproduced with permission.[14] Copyright 2003, Elsevier.
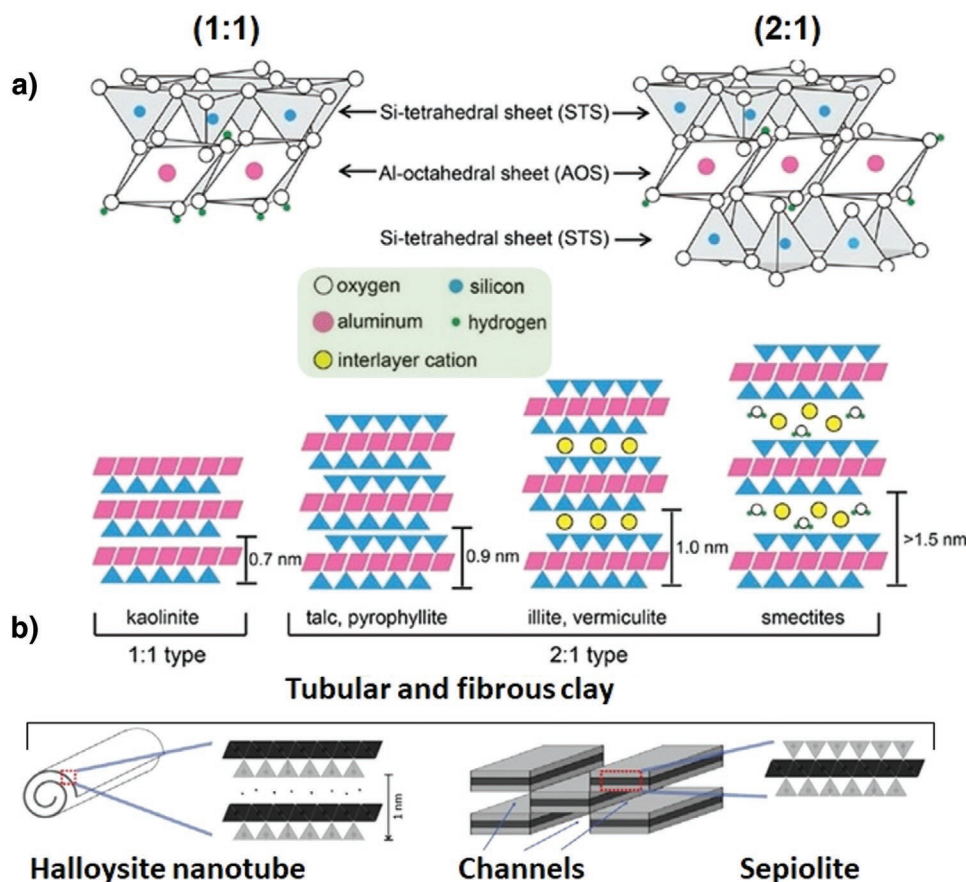
Figure 2. Various clay architectures and their unit cells: All clays represent layered silica tetrahedral (T) and alumina octahedral (O) sheets. The ratio between T and O sheets varies for each clay. a) The kaolinite family has a 1:1 ratio of T and O sheets. Pyrophyllite, vermiculite, and smectite families comprise two tetrahedral sheets sandwiching an octahedral sheet (2:1 ratio of T and O) along with Al^{3+} or Mg^{2+} exchangeable cations. These minor variances in the crystal structure greatly influence the colloidal properties and stacking arrangements. b) Fibrous structure with channels and tubular-like morphology of halloysite and sepiolite nanoclay families, respectively. 1:1 ratio of T and O sheets are rolled up to form a nanotube-like structure in case of halloysite nanoclay. The tubes have a length between 0.2 and 1.5 μm with an outer diameter of a 50 nm and an inner diameter of a 15 nm. Sepiolite clay has a 2:1 ratio of T and O sheets forming needle-like structures with channels. It has a high aspect ratio with a length of ≈0.3 to 3 mm, a diameter of 15–25 mm along with a thickness of less than 10 nm. a) Reproduced with permission.[23] Copyright 2019, Wiley-VCH. b) Reproduced with permission.[19] Copyright 2018, Elsevier.

nanocomposite morphologies such as thin films, fiber meshes, hydrogels and 3D scaffolds for potential biomedical applications.

2. Clay Composition and Architecture

Most clays are derived from alkaline volcanic ash by hydrothermal processing. Clays are composed of extremely fine crystals of mixed metal ions. They are mainly based on phyllosilicates, for example, hydrous silicates of aluminum (Al), zinc (Zn), magnesium (Mg), iron (Fe), and less on other metal ions.[23] The microstructure of clays is often observed in a platelet fashion having less than 2 μm in diameter and less than 10 nm in thickness. Additionally, each layer comprises at least one silica (SiO_2) tetrahedron (T) followed by one alumina (Al_2O_3) octahedron (O). The number of tetrahedron (T) and octahedron (O) units may differ between clays. Clays are often categorized on the basis of their crystal architecture as well as the amount and location of a charge within a basic cell,

cation exchange capacity (CEC), the ratio of T and O units, interlayer space (d-space) and morphology.[24] However, the majority of the fashionable clay minerals used for the reinforcement of copolymers are the following types: laponite, layered double hydroxide, montmorillonite, halloysite, and sepiolite. Clay families and their architecture, morphology and chemical composition are shown in **Figure 2** and **Table 1**, and selected families are introduced in more details below.

2.1. Kaolinite/Kaolin Family

This family comprises three subfamilies namely kaolinite, dickite, and nacrite.[25] The chemical composition of kaolinite clay shows more (%) alumina content than silica. The typical chemical formula of kaolinite clay is $Al_2[Si_2O_5](OH)_4$. The crystal structure consists of multiple layers made up of tetrahedral sheets (T) in which silicon is surrounded by four oxygen atoms, and octahedral alumina sheets (O) are surrounded by

Table 1. Various clays and their properties. (Data from refs. [19,23]).

Ratio	Group	Species	Chemical formula	Distance between adjacent layers [10^{-1} nm]	CEC [meq/100 g][a]	Morphology and particle size
1:1	Serpentine-kaolin	Halloysite	$Al_2Si_2O_5(OH)_4 \cdot 2H_2O$	7.2	≈10	Nanotube diameter of ≈50 nm; lumen ≈15 nm; length ≈1 µm
2:1	Smectites	Montmorillonite	$Si_{12}Mg_8O_{30}(OH)_4(OH_2)_4 \cdot 8H_2O$	70–130	≈80–150	Diameter of ≈80–300 nm and thickness of ≈1 nm
		Laponite (synthetic hectorite)	$Na^{+0.7}[(Si_8Mg_{5.5}Li_{0.3})O_{20}(OH)_4]^{-0.7}$			Diameter of ≈25–30 nm and thickness of ≈1 nm
	Sepiolite-palygorskite	Sepiolite	$Si_{12}Mg_8O_{30}(OH)_4(OH_2)_4 \cdot 8H_2O$	20–40	≈4–40	Diameter of ≈15 nm; length ≈200–400 nm

[a]CEC: cation exchange capacity and meq: milliequivalent.

eight oxygen atoms in the ratio of 1:1.[2,26] Layers are packed toward the c-axis. The distance between the layers is ≈0.71 nm. The kaolinite nanoclay has a low cation exchange capacity that challenges the intercalation of any molecule or polymer chain into the gallery of nanoclay. Additionally, the interlayer H bonding between layers is very strong.[2] These characteristics suggest that kaolinite is not a good candidate for nanocomposites,[27] but it is a potential filler for paint and food packaging applications.[28] The majority of the applications are in paper industry to produce glossy paper.

2.2. Halloysite Family

Halloysite family clays are naturally available and show a tube-shaped structure with a high aspect ratio of ≈19 (Figure 2b). The tube has an outer diameter of ≈50 nm, and an inner diameter of 15 nm along with a length of 0.2–1.5 µm.[29] The chemical composition of halloysite is similar to that of kaolinite with the difference that there is an extra water monolayer between the two silicon tetroxide and aluminate layers. The empirical formula of halloysite nanotube is $Al_2Si_2O_5(OH)_4 \cdot 2H_2O$. Most importantly, halloysite clay does not require any exfoliation during the composite fabrication due to the hollow shape of the clay i.e., (absence of stacked layers). The porous and hollow structures are capable of interacting well with polymer chains and provide a strong bonding. Besides that, halloysite is more hydrophilic than other clays.[30] Hence, it can be well dispersed in water and it is more biocompatible compared to other clays. Owing to its unique architecture of a hollow structure with pores, it can be used for targeted drug delivery.[31] However, it is also used as a flame retardant agent in composite product manufacturing, since it can bind a large amount of water.

2.3. MMT Family

MMT is the clay family mostly used for the preparation of copolymer nanocomposites.[32] It combines many minerals mainly talc, saponite, pyrophyllite, etc. It has a very small quantity of Al_2O_3 moieties and a large quantity of SiO_2. The microstructure of MMT possesses a distinctive layered platelet morphology with a sandwiched structure of an edge-shared octahedral plate of Al_2O_3 and fused type of SiO_2 with the ratio of 1:2[33] and a

thickness of close to 1 nm. According to the specific layered silicate, the sidewall (thickness) of the clay varies from 30 nm to µm or even more. External molecules or water can penetrate it easily, and the lattice will then expand significantly. Therefore, the $d_{(001)}$ space or gap between each layer increases, which will be beneficial for penetration with polymer chains.[34] Partially or completely intercalated and exfoliated clay morphologies can be achieved for the fabrication of polymer/clay nanocomposites. MMT is also capable to exfoliate into 3D tactoids after nanocomposite preparation. Furthermore, sepiolite is also a part of the MMT family and composed of hydrated magnesium silicate, $Si_{12}Mg_8O_{30}(OH)_4(OH_2)_4 \cdot 8H_2O$.[35] Sepiolite architecture is similar to that of MMT with tiny variations in its morphology i.e., (shape). The fibrous or needle-like structure has a length of ≈0.3 to 3 mm, a width of 15–25 mm along with a thickness >10 nm and a microporosity with the size of 0.37–1.06 nm^2 (Figure 2b). It also has a high surface area of 300 m^2 g^{-1} compared to that of other types of nanoclay.[36] Due to the hollow fibrous structure, it is useful for drug encapsulation. Additionally, these hollow channels can absorb polymer chains which can integrate with good interfacial adhesion.

2.4. Laponite Family

Laponite is a synthetic clay with a layered silicate disc type structure forming less strongly layered structures than natural silicates. $Na^{+0.7}[(Si_8Mg_{5.5}Li_{0.3})O_{20}(OH)_4]^{-0.7}$ is the typical chemical composition of laponite nanoclay and it appears as diskettes shape.[37] The diameter of diskettes varies from 25 to 30 nm, with 1 nm thickness. The crystal size of the laponite is smaller than that of the MMT family. The size of laponite nearly matches the dimensions of phase-separated hard domains present in many copolymers, such as polyurethane.[38]

2.5. Layered Double Hydroxide Clays

LDH is also a type of nanoclay but it is not naturally available. LDH is anionic with unique layered structures. It is referred to as hydrotalcite and has a large amount of bound water in its interlayer space. $[M^{2+}_{(1-X)}+M^{3+}_{(X)}(OH)_2]X^+(An^-)_{X/n} \cdot mH_2O$ is the chemical composition of LDH, where M^{2+} and M^{3+} denotes the divalent and trivalent metallic cations, respectively. An^- signifies

an anion and X is fraction constant ($M^{3+}/M^{3+}M^{2+}$) in the range of between 0.22 and 0.33.[39] Combined trivalent and divalent cations make LDH positively charged sheets (hydrophilic) that can offer a wide range of organic modifiers selection according to their functional groups, such as carboxyl, ester, epoxy, phosphoryl, etc. and different modification techniques including in situ synthesis, electron beam, surface grafting, ionic liquid).[40] LDH is also widely used in catalysis for polymer synthesis, as a stabilizer, in medical materials, as superabsorbent, in ion exchangers or as DNA reservoir.[41]

2.6. CEC of Clays

Cation exchange capacity is an important feature of clays as it can predict the dispersion characteristics of nanoclays in copolymer matrices. CEC can influence the degree of intercalation or exfoliation morphology of composites with copolymers. CEC describes how much cations the clay are capable to hold at a certain pH value.[42] It is expressed as centimol per kg (cmol kg^{-1}) or milliequivalent of hydrogen per 100 g (meq/100 g). The electrostatic interaction between the clay platelets plays a role, too. If the surface charge is negative (−), then a nanoclay has strong hydration characteristics as well as better swelling capabilities, which are beneficial for penetration with polymer chains.[43]

2.7. Surface Modifications of Clays

Layered silicates can be intercalated with hydrophilic polymers such as poly(vinyl alcohol) (PVA), poly(ethylene glycol) (PEG), poly(acrylic acid) (PAA), poly(2-oxazoline) (POX), poly(methyl methacrylate) (PMMA) and poly (ethylene-*co*-vinyl acetate) (EVA), but most of the used polymers are hydrophobic. For compounding layered silicates with engineering polymers such as nylon or polyethylene–octene, the surfaces of the layered silicate have to be modified by ion-exchange processes using cationic surfactants like alkylammonium or alkylphosphonium-based positively charged species. Such motifs reduce the surface energy of the inorganic host. As a result, the larger interlayer spacing increases, yielding better anchoring of the polymer chains for improving the technical properties of the nanocomposites. The significant increment in the interlayer distance (d-space) of the organically modified nanoclay can be observed using X-ray diffraction (XRD).[44] The peak 2θ value of the modified clay has to shift to a lower degree compared to that of pristine MMT, which means that the *d*-value increased according to Bragg's law. The mechanical stability, such as tensile strength and modulus of the fabricated polyurethane copolymer/organically modified MMT (OMMT) composites was improved significantly in comparison to that of unmodified MMT.
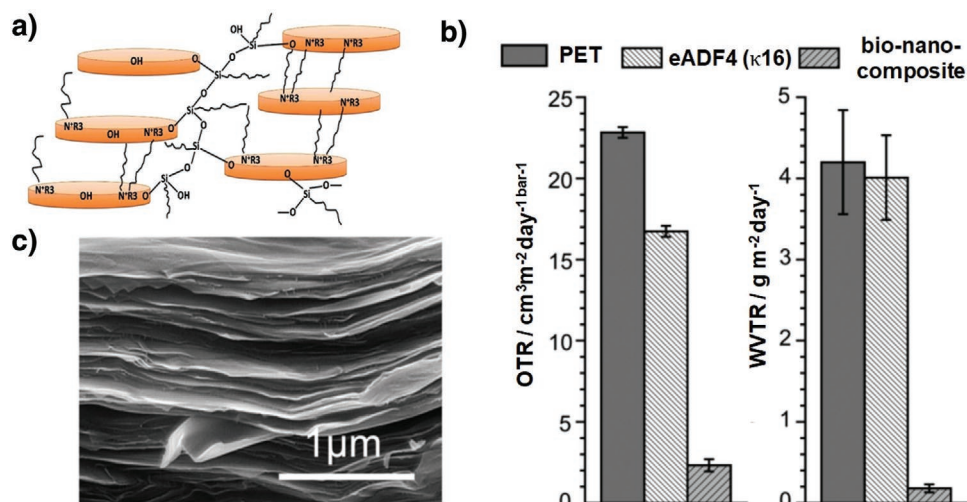
Besides ionic modifications, covalent and dual modifications (ionic and covalent) are feasible.[45] Other approaches, such as grafting polymer chains directly onto the surface of a nanoclay[46] or using non-ionic surfactant have also been used. There are two ways of ionic modification, namely directly reacting anionic or cationic surfactants with the nanoclay or using ionic liquids. Often ionic liquid-modified clays show better properties than other ones.[47] Imidazolium, pyridinium, trihexyltetradecylphosphonium tetrafluoroborate, and trihexyltetradecylphosphonium decanoate salts are commonly used for ionic liquid modification of nanoclays.[48] Modesti et al.[49] improved the thermal insulating properties of polyurethane-MMT nanocomposite foams by incorporating imidazolium salt modified MMT. Ha et al.[50] used 1-ethyl-3-methylimidazolium bromide to modify MMT-Na$^+$ clay in aqueous solution: Anionic/cationic surfactants such as dodecyl ammonium ions, cetyltrimethylammonium ions, and cetyltrimethylammonium bromide have been widely used in copolymer chemistry, as these surfactants can further react with the polymers, thus, improving the interaction between the nanoclays and the copolymer matrix.[9a,35,36,51]

Covalently modified silicate is often synthesized using a condensation reaction of the hydroxyl groups from the surface of clays with mono- or tri-alkoxy silanes, for example, methoxy(dimethyl)octylsilane, tri-alkoxy silanes, trimethoxy(octyl)silane, (3-aminopropyl) triethoxysilane, etc. The covalent modification renders the clay surface more hydrophobic.[38b,53] Mishra et al.[38b] studied the structure–property relationship of composites comprising polyurethane and covalently modified laponite. The laponite/polyurethane nanocomposite exhibited a higher storage modulus and a significant improvement in thermal properties than pristine polyurethane, as the nanoclay acted as a radical scavenger. Covalent modification of nanoclays can also be done by grafting reactions using methylene di-isocyanates.[53b]

Dual modifications can be done by first covalently modifying the clay followed by ionic modification or vice versa. In comparison to single modifications (either ionic or covalent), du ally modified clays show even more improved properties in terms of mechanics,[38] thermal stability,[38a,54] dimensional stability,[38a] and viscoelastic characteristics.[38a,54] Mishra et al.[38b,45] and Mondal et al.[38a,54,55] reported on dually modified laponite compounded with segmented polyurethane-based copolymers. They first performed an ionic modification of laponite followed by covalent modifications. The structure of dual modified laponite is shown in **Figure 3**a according to the interpretation of spectra obtained using solid-state Si-nuclear magnetic resonance (NMR) and Fourier transform infrared spectroscopy (FTIR).

Modification using biomolecules/proteins have been also explored to enhance the biological or other properties of the nanoclay. Doblhofer et al.[52] reported on the preparation of L-lysin modified sodium-fluorohectorite nanoclay for the fabrication of layer-by-layer stacked multilayer nanocomposite films using spider silk proteins as a matrix in an aqueous medium. The film thickness or number of layers was controlled by multiple drop-casting steps. The prepared multilayers showed a highly ordered lamellar structure and excellent water vapor barrier properties (Figure 3b), reduced rate of thermal degradation, and enhanced tensile strength as compared to pristine spider silk protein films. The % improvement of the barrier properties and field emission scanning electron microscope (FESEM) microstructure of the lamellar surface morphology of the prepared multilayer film (cross-sectional view) are depicted in Figure 3b,c.

**ADVANCED
SCIENCE NEWS**

www.advancedsciencenews.com

**ADVANCED
FUNCTIONAL
MATERIALS**

www.afm-journal.de

Figure 3. a) Schematic representation of dual modified laponite clay platelets using hexadecyl trimethyl ammonium bromide (ionic) followed by octyl trimethoxy silane (covalent) treatment. b) Oxygen and water vapor transmission rate of films (spider silk, clay/spider silk nanocomposite and PET film, and c) FESEM surface morphology of a fabricated layer-by-layer lamellar film. a) Reproduced with permission.[38b] Copyright 2011, American Scientific Publishers. b,c) Reproduced with permission.[52] Copyright 2016, ACS.

3. Polymer Composition

Polymers are mainly classified in three categories such as thermoplastics, thermosets, and elastomers based on the absence or presence of crosslinking rendering the polymers meltable (thermoplasts) or not (thermosets).[56] Generally, Polymers can be categorized according to the structure. Amorphous polymers show a low density, with polymer chains oriented irregularly. Crystalline polymers show high density and the polymer chains are oriented in a regular manner yielding good mechanical strength. Amorphous polymers, in contrast, provide more than 300% elongation. One can obtain a desired mechanical property, e.g., by tuning the crystallinity of the polymer. Characteristics of polymers are further controlled by their chemical setup including a) homopolymers, b) copolymers, c) star polymers, and d) dendrimers.[57] A homopolymer comprises a chain of single monomers, which means the properties of the polymer are depending on the structure of an individual repeating unit. Copolymers, star polymers, and dendrimers comprise a minimum of two different monomers, which means that the polymer properties depend on several features or one can adjust the properties by choosing the desired mole % of each monomer. Compared to a homopolymer, copolymers are widely used in biomedical applications due to their tailor-made characteristics including a degree of hydrophilicity, capability to be processed into several shapes/morphologies, biocompatibility, biodegradability and mechanical properties.[58] **Table 2** displays the chemical structures of tailor-made synthetic copolymers used in biomedical applications.

4. Biomedical Applications of Copolymer/Clay Nanocomposites

Clay/copolymer nanocomposites can be processed into 2D and 3D morphologies such as thin films, fiber scaffolds, hydrogels,

and bioinks for 3D bioprinting, (**Figure 4**). Biomedical applications of such copolymer/clay nanocomposites are briefly discussed in the subsequent sections.

4.1. Copolymer/Clay Films

Fabrication of thin-films is the best choice to study the mechanical properties or biological activities of any designed nanocomposite.[78] Clay/copolymer nanocomposite films can be fabricated using solution casting, melt mixing and in situ intercalative approaches.[79] These techniques require small quantities of raw materials or monomers. The surface roughness/topography, functionalities, and stiffness of the film can be tuned by the fabrication technique as well as by post-treatment of the prepared films.[59,80] In a simple and cost-effective approach, the polymer is dissolved in a suitable solvent along with the clay. Alternatively, the copolymer and the clay are separately dissolved in a solvent. There, the clay is stirred under ultrasonic vibration to avoid the formation of aggregates and obtaining a better dispersion.[79] This solution is then added slowly to the polymer one. Sometimes, the entire mixtures (polymer+clay+solvent) are again sonicated to obtain a better homogeneity. Finally, the solution is transferred to the desired mold, and the solvent evaporates. Several studies have been reported on the solution blending of copolymer/clay nanocomposites.[23,52,65,71,81] The solution cast films are used as drug delivery patches, biodegradable/biocompatible packaging films, packets for storing blood, and various microfluidic devices.

The in situ intercalative polymerization technique is also used to fabricate a copolymer/clay nanocomposite thin film, and first successful attempts were made using this approach with a nylon6 matrix.[14,26] Modified Na+-MMT was incubated with 1-caprolactam monomer overnight. Then, the ring-opening polymerization was begun either by heat or radiation to produce nylon6/MMT nanocomposites.[14] This processing

**ADVANCED
SCIENCE NEWS**
www.advancedsciencenews.com

**ADVANCED
FUNCTIONAL
MATERIALS**
www.afm-journal.de

Table 2. Chemical structures of tailor-made synthetic copolymers used for the preparation of nanocomposites with nanoclays for various biomedical applications.

Copolymer name	Chemical structure (repeating unit)
Polyurethane based on polytetramethylene oxide (PTMO) soft segments[69]	
Polyurethane based on polycaprolactone diol soft segments[70]	
Poly-3-hydroxybutyrate-*co*-3-hydroxyvalerate (PHBV)[71]	
Thermoplastic polyurethane based on silicone soft segments[72]	
Poly (methyl methacrylate-*co*-methacrylic acid)[73]	
Poly(lactide-*co*-glycolide)[60,67,74]	
Poly(acrylic acid-*co*-N-isopropyl acrylamide)[75]	
Poly(N-isopropyl acrylamide-*co*-acrylamide)[76]	
Poly (acrylamide-*co*-sodium acrylate)[77]	

method requires more time compared to others, and reaction time, efficiency and quality of the end product depend upon factors such as polarity/functional group of the used monomer, the functional group of the clay and temperature at which the reaction is carried out. A slightly modified process combines ring-opening polymerization and "click" chemistry to fabricate copolymer/clay nanocomposites.[82] Poly(styrene-*block*-tetrahydrofuran)/azide-functionalised montmorillonite based nanocomposite films were fabricated by cationic ring-opening polymerization combined with click chemistry (for surface
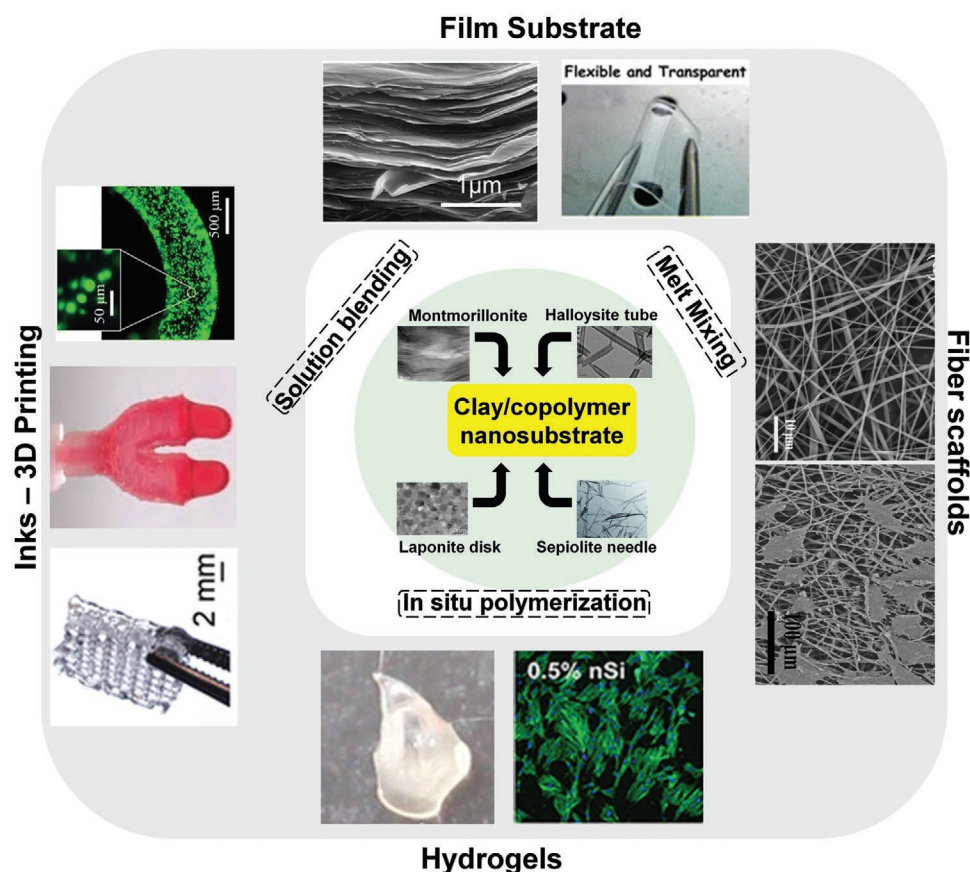
Figure 4. Clay/copolymer nanocomposites used for biomedical applications. Various nanoclays have been employed for the development of copolymer nanocomposites using solution blending, melt mixing, electrospinning and 3D biofabrication yielding films, fiber mesh scaffolds, hydrogels and 3D constructs. (Individual parts reproduced with permission:[52] Copyright 2016, American Chemical Society (ACS);[59] Copyright 2014, ACS;[60] Copyright 2012, ACS;[61] Copyright 2014, Wiley-VCH;[62] Copyright 2018, ACS;[63] Copyright 2018, ACS;[64] Copyright 2018, ACS;[65] Copyright 2018, ACS;[66] Copyright 2016, Royal Society of Chemistry (RSC);[67] Copyright 2010, RSC;[5a] Copyright 2015, IOP Publishing;[68] Copyright 2018, Wiley-VCH).

modification of MMT).[83] Azide-functionalized montmorillonite clay surface-initiated ring-opening polymerization and click chemistry was also used for the fabrication of poly(ε-caprolactone) nanocomposites to improve the mechanical as well as thermal stability by inducing the polymer-filler interaction and obtaining better intercalated/exfoliated structures.[84]

Lastly, melt intercalation is another technique for preparing copolymer/clay nanocomposite films using various types of mixing such as extrusion, co-rotating using twin-screw mini extruder, blow molding, etc. First, the copolymer is melted and then the clay incorporated into the molten polymer. Sometimes, annealing slightly above the glass transition temperature (T_g) of the polymer is necessary to promote the nanodispersion of the filler. The benefit in comparison to in situ intercalative polymerization and solution intercalation is the higher degree of intercalation or exfoliation. Furthermore, it is more compatible with current industrial processes.[85] The melt mixing technique is mainly used to fabricate a larger quantity with greater sizes like hard tissue implants[86] and flexible pads to support and recover the strained tissues during injuries, such as knee pads. Nanoclay-incorporated copolymer films own outstanding mechanical properties, shape memory characteristics, biodegradability, optical transparency, antimicrobial activity, and gas barrier properties, etc.[87] There are many reports on copolymer/clay nanocomposite films used for biomedical applications and they are summarized in **Table 3**. Recent results from various reports are discussed below.

Clay/copolymer nanocomposite films are frequently used in drug delivery applications as they provide mechanical support, and the quantity of filler, shape of nanoclay, aspect ratio, degree of intercalation/exfoliation, and the ionic strength of the clay can be tailor-made according to the drug properties before incorporating the clay into copolymer matrices.[88] Among the mechanisms to describe drug release from nanocomposites, the tortuous pathway model is the most appropriate one (**Figure 5**a).[13,40,69,81b] Compared to other morphologies like micelles, capsules, nanogels, vesicles, etc., the films are more stable (mechanically and chemically), which supports the release of the drug for a longer time. Chung et al.[69] studied the relationship between various organically modified clays using dodecylamine-MMT and hexadecylamine-MMT reinforced polyurethane copolymer films.[69] The degree of intercalation was further enhanced after addition of drugs, which indicates that the drug has entered between the gallery spaces of the nanoclay. The drug release profiles relied on the charge of drugs, drug size, gallery space, and degree of intercalation

**Table 3.** Clay/copolymer-based films and their biomedical applications.

Polymer	Clay type/technique used for the preparation of films	Features	Cell line and cytotoxicity evaluation (if available)	Application
Polyurethane based on polytetramethylene oxide (PTMO) soft segments[69]	Montmorillonite as well as organo-montmorillonite using dodecylamine and hexadecylamine/solution casting	The drug release profile depends on key factors such as filler-polymer interaction, drug surface charge, and functionalities. The rate of drug release from nanocomposite film decreased for positively charged drugs and it increased for negatively charged drugs, when the d-space of the nanoclay increased.	–	Drug delivery
Polyurethane based on polycaprolactone diol soft segments[102]	Methyl tallow bis-hydroxyethyl quaternary ammonium ion-exchanged montmorillonite, layered double hydroxide of Mg–Al–NO$_3$/in situ polymerization followed by solution casting	Organic modification enhanced the dispersion characteristics and thermal stability of the copolymer. All nanocomposite films showed shape memory properties capable to change their shapes into coil, spinal and straight strips at different temperature.	–	Smart robotics
Polyurethane based on polycaprolactone diol soft segments[89]	Montmorillonite clay/ex situ casting	Nanoclay improved the mechanical strength of the film. The nanocomposite films promoted sustained drug release characteristics (up to 371 days), which implied that the clay incorporation slowed the rate of polymer degradation by hydrolysis.	Human retinal pigment epithelial cells (ARPE-19)	Retina regeneration
Poly (2-hydroxyethyl methacrylate)-co-poly(ethylene glycol) dimethacrylate[103]	Hyperbranched polymer, polyethyleneimine-co-polyesteramide modified montmorillonite clay/casting	Hyper branch modification of MMT clay enhanced the degree of intercalated/exfoliated structures of nanocomposites. Thermal stability improved upon addition of the organoclay. Nanocomposite films significantly inhibited growth of Bacillus subtilis and Pseudomonas aeruginosa.		Antimicrobial coatings
Poly-3-hydroxybutyrate-co-3-hydroxyvalerate (PHBV)[71]	Vinyl triethoxy silane-grafted sepiolite clay/solution casting	Thermal stability and mechanical properties (tensile strength and young's modulus) increased significantly with the incorporation of organoclay.	–	Biodegradable implants
Commercial biomedical grade PU (pellethane 2363–80A) having polytetramethylene oxide (PTMO) as a soft segment[104]	A cationic, nonionic, and an anionic surfactant such as sodium dodecyl sulfate, triton X-100 and n-octadecanylamine hydrochloride salt modified montmorillonite clay/solution casting	All types of organo clay nanocomposites showed higher surface roughness of the film at higher clay loading, less cytotoxicity and faster cell proliferation. Cationic and anionic clays showed excellent antimicrobial characteristics against Gram-negative bacteria.	Bovine carotid arterial endothelial cells and Human skin fibroblasts	Skin tissue engineering
Thermoplastic polyurethane based on silicone soft segments[72]	Dual-modified synthetic hectorite clay (lucentite) with the varied polarity of quaternary alkyl ammonium salts (dimethyl dioctadecyl ammonium chloride/cholinechloride)/solution casting	The nanocomposite showed significant improvement in mechanical properties, reduced thermal degradation, and retention of tensile strength as well modulus even after oxidative treatment. Biostability of the nanocomposites considerably increased compared to that of pristine polyurethane copolymer film.	–	Long-term implantable medical devices
Thermoplastic polyurethane based on aromatic polyether soft segments[81b]	Sodium montmorillonite/solution casting and electrospinning	The electrospun mat displayed higher drug release rate than the cast films. All drug loaded samples showed good zone of inhibition against pathogens.	–	Wound healing
Cellulose-graft-poly(butyl acrylate)[99]	Kaolin clay/in situ polymerization followed by solution casting	Improved thermal stability, and mechanical properties were obtained for the nanocomposite films. Limiting oxygen index (LOI for flammability characteristics) and % char residue from TGA were increased with the clay reinforcement content. Biodegradation and % water absorption increased with the % nanoclay loading.	–	Biodegradable medical devices
Hyperbranched epoxy[55b]	Octadecylamine-modified montmorillonite and H. aromatica oil modified bentonite/in situ solution polymerization	Prepared nanocomposite showed high impact resistance, scratch hardness, tensile strength, and % elongation. Nanocomposite film also showed good compatibility with cell as well as blood, excellent antimicrobial activity, and showed no acute toxicity in the rat model.	Mammalian red blood cells, cell viability was higher than 90%	Implants
Silk fibroin Bombyx mori silkworm white cocoons[59]	Hydrotalcite clay/solution casting	The clay content did not affect the conformational properties of the silk protein films. Optical characteristics, mechanical strength, and % water absorption and acidic environment resistance were enhanced upon addition of nanoclay.	–	Opto-electronic and photonic devices
Poly(hydroxybutyrate-co-valerate)[70]	Methyl tallow bishydroxyethyl quaternary ammonium cation and di-methyl dihydrogenated tallow ammonium cation modified MMT/solution casting	Nanocomposite showed an improved biodegradation. The different nanoclays affected the crystallizing behavior of the copolymer matrix.	SiHa cells, cell viability was nearly 100%	Drug delivery and bone tissue engineering

1908101 (9 of 28)

Table 3. Continued.

Polymer	Clay type/technique used for the preparation of films	Features	Cell line and cytotoxicity evaluation (if available)	Application
Poly(hydroxybutyrate-co-hydroxyvalerate)[105]	Monotallow bis-hydroxyethyl ammonium-modified montmorillonite clay/melt blending followed by compression molding	Partially exfoliated organoclay improved the crystallization of copolymer, tensile properties and thermal stability.	–	Hard tissue implants
Poly(tetramethylene oxide) based soft segments of poly(ether)urethane[100]	Organo MMT, chlorhexidine diacetate drug modified MMT[106]/solution casting	Nanocomposite films showed an excellent antibacterial activity against Staphylococcus epidermidis in an in vitro urinary tract (UT) model with prolonged drug release.	–	Catheter-related nosocomial infection
Poly(dimethyl siloxane/hexamethylene oxide) based soft segments of polyurethane (ElastEon E5325)[72]	Polar and nonpolar quaternary alkyl ammonium modified hectorite nanoclay/solution casting	Exfoliated clay nanocomposite films displayed outstanding mechanical properties even after induced oxidation.	–	Long-term implants
Poly(ether)urethane based on poly (tetramethylene oxide) soft segments[107]	Amino undecanoic acid and quaternary ammonium modified MMT/in situ solution polymerization followed by casting	Delaminated clay nanocomposites demonstrated a good in vivo stability in an ovine model for a 6-week time interval, and no inflammatory response was observed from the stained histological sections.	–	Long-term implants
Poly(tetramethylene glycol) based soft segments of polyurethane[90,108]	Methyl tallow bis-hydroxyethyl quaternary ammonium ion modified MMT/in situ solution polymerization followed by casting	Significant improvement was observed in toughness and strength of the films upon addition of nanoclay. The nanocomposite films also presented better cell compatibility and proliferation rate.	Epithelial cells, SiHa and HeLa cells. cell viability was nearly 90% for all cells	Tissue regeneration as well as angiogenesis therapy
Silk from Bombyx mori cocoons[109]	Sodium modified montmorillonite/solution casting	About 95% cell confluence was observed after 2 weeks for the hybrid films. The improved transcript levels for alkaline phosphatase (ALP), bone sialoprotein, and collagen type I were evidence for the excellent differentiation capability of the nanocomposite films.	Human bone marrow derived mesenchymal stem cells cell viability was 95%	Bone tissue engineering

or exfoliation. However, the organically modified clay nanocomposite enabled to encapsulate a large amount of drug and a controlled release up to 800 h.[69] In a separate study, dexamethasone acetate embedded in a poly(caprolactone)-based soft segment polyurethane/MMT nanocomposite film was used for treatment of uveitis.[89] The drug and nanocomposite interaction was strong via hydrogen bond formation as evidenced from the shift of the carbonyl peak toward lower wavenumbers (FTIR). Small-angle X-ray scattering (SAXS) confirmed that the nanoclay was preferentially interacting with the hard segment of the PU copolymer leading to additional reinforcement of the nanocomposite film. The drug embedded nanocomposite film was biocompatible as evidenced by the adhesion of a human retinal pigment epithelial cell monolayer after 7 days of culturing. There are other reports, which provided insight into the improvement of biodegradability, cell metabolic activity, release characteristics, microbial protection, equilibrium swelling, in vivo biocompatibility with minimal inflammation, and mechanical properties of various copolymer/nanoclay composite films. Examples are chlorhexidine acetate loaded PU/MMT films,[81b] laponite/mafenide/alginate films,[90] sulfamethoxazole and diclofenac sodium embedded polyester polyol acrylate/bentonite nanocomposite films[91] and soy protein/MMT films for ofloxacin drug release.[92] The above-mentioned findings suggested that the intercalated nanoclay morphology is capable of loading high amounts of drug and yielding a more prolonged release compared to that of the exfoliated structure. The reason is that the average drug travel path distance is shorter and easier within the exfoliated one (Figure 5a). Among different clays, organo-MMT has been used more frequently for the preparation of nanocomposite free-standing films to use them as drug delivery carrier. Higher drug loading efficiencies combined with higher strength are achieved with organo-MMT, since they provide larger interlayer spacings in which the drug molecules can enter more efficiently. Halloysite is also used due to its hollow architecture enabling incorporation of a high amount of drugs.[93]

There are few studies on exfoliated structures offering higher mechanical strength for the nanocomposite film compared to the intercalated structures. Mishra et al.[38b] reported on in situ prepared dual modified (ionic and covalent) laponite strengthened polyurethane nanocomposite films to improve the technical properties. High-resolution transmission electron microscopy (HRTEM) morphology revealed that dual modification yielded a more exfoliated structure and led to substantial enhancement of the tensile strength, storage modulus and onset of the thermal degradation temperature compared to the intercalated structure (single modification). Figure 5b displays the intercalated (single modification, right picture) as well as exfoliated (dual modification, left picture) laponite nanodisks in a PU copolymer matrix. Other copolymer matrix/clay nanocomposites such as poly(3-hydroxybutyrate-co-3-hydroxyhexanoate)/organo MMT,[94] soy proteins reinforced by montmorillonite,[80] bentonite reinforced waterborne polyurethane,[95] biocomposites of soy proteins/organo MMT[96] and biodegradable poly (3-hydroxybutyrate-co-3-hydroxyhexanoate) and silane-modified kaolinite/silica dual filler[97] were used for improving thermal stability, mechanical strength including dynamic mechanical properties, cell viability, and rate of cell proliferation. In another report, Silvestri et al.[98] examined the shape
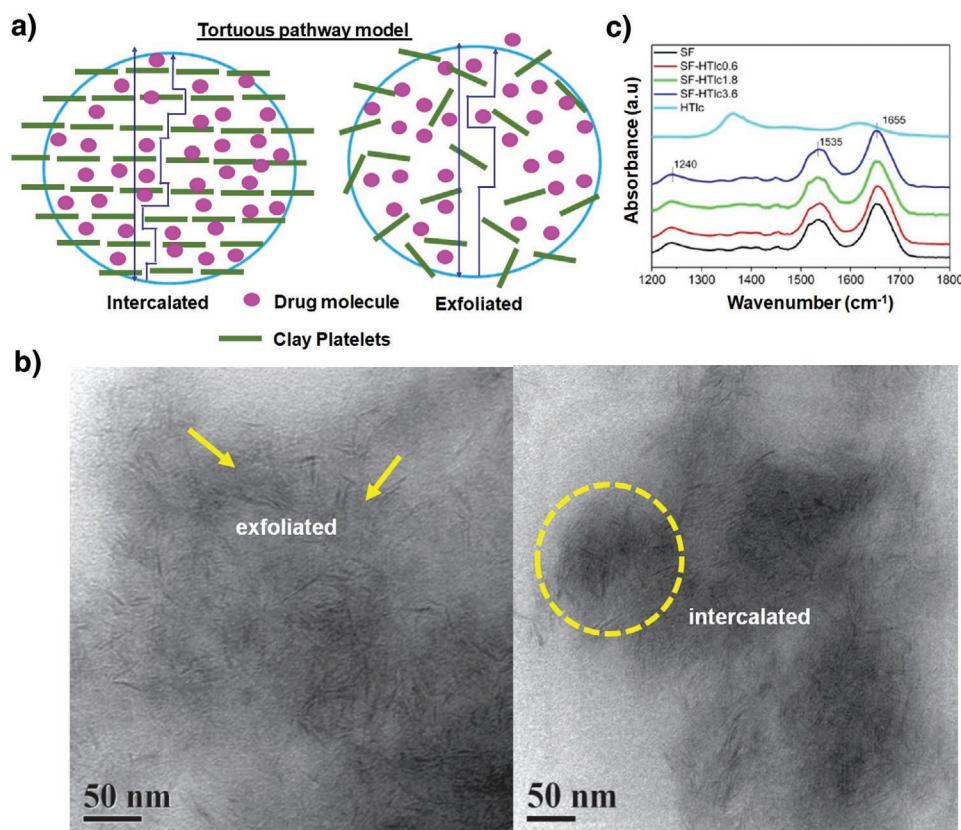
Figure 5. a) Tortuous diffusion pathway model showing an intercalated clay/copolymer nanocomposite with prolonged drug release as well as good barrier properties in comparison to a less performing exfoliated one. b) High-resolution transmission electron microscope micrographs of intercalated (single modification, right picture) as well as exfoliated (dual modification, left picture) laponite nanodisks in a polyurethane copolymer matrix. c) FTIR spectroscopy unveiled hydrotalcite nanoclay incorporation (0.6 to 3.6 wt%), which did not alter the secondary structure of the silk fibroin matrix in a nanocomposite film. a) Adapted with permission.[38b] Copyright American Scientific Publishers. b,c) Reproduced with permission.[59] Copyright 2014, ACS.

memory properties of in situ prepared organo MMT incorporated ether and silicone-based polyurethane nanocomposites for fabricating cardiovascular surgical implants. Improved shape memory or recovery of the nanocomposite films were examined using various modes of mechanical testing such as creep, tensile and fatigue measurements. The prepared composite films were favorable substrates for mouse fibroblasts. Improved biodegradability combined with fire resistance of cellulose-*graft*-poly(butyl acrylate) upon kaolin platelet reinforcement was reported by Jena and Sahoo.[99] Additionally, several features were achieved such as increased mass loss after biodegradation, reduced time to ignition (TTI), reduced mass loss rate (MLR), increased char yield (%) from the cone calorimetry test, and increased limiting oxygen index of the copolymer upon addition of kaolin up to 5 wt%. Fong et al.[100] reported on chlorhexidine diacetate antiseptic drug modified MMT reinforced polyurethane nanocomposite thin films with improved mechanical properties combined with antimicrobial characteristics. The bacterial adhesion was reduced in case of chemically attaching the drug compared to that of physical loading. In a separate study, properties were improved such as tensile strength, cell viability, and biodegradation without compromising the optical transparency of silk fibroin *Bombyx mori* silkworm film upon compounding it with hydrotalcite. The

addition of nanoclay did not alter the secondary structure of the silk proteins, which was confirmed using FTIR spectroscopy (Figure 5c) as there was no change in the peak position/area of Amide-I (1655 cm^{-1}), Amide-II (1535 cm^{-1}), and Amide-III (1240 cm^{-1}) and wide-angle X-ray diffraction. The optical transparency of the silk protein films was retained even at 3.6 wt% nanoclay reinforcement. Similarly, the structure–property relationship of cationic recombinant spider silk protein (spidroin) eADF4(κ16)/lysine modified sodium hectorite nanocomposite film was studied.[52] The prepared silk nanocomposite films were very stable (mechanically as well as chemically) yielding high oxygen and water vapor barrier properties. The barrier properties were 600-fold and 60-fold higher compared to that of commercial packaging polymers such as poly (ethylene terephthalate) (PET) and poly(vinylidene chloride) (PVDC), respectively. Improved biodegradation and barrier properties of starch-based copolymer-aliphatic polyester/starch blend films were achieved upon organo MMT reinforcement (5%).[101] Singh et al.[70] demonstrated that methyl tallow bishydroxyethyl quaternary ammonium cation and di-methyl dihydrogenated tallow ammonium cation modified MMT clay incorporated in poly(hydroxybutyrate-*co*-valerate) nanocomposite films increased their properties like cell adherence, biodegradation, mechanically durability, and controlled drug release. Overall,

**ADVANCED
SCIENCE NEWS**
www.advancedsciencenews.com

**ADVANCED
FUNCTIONAL
MATERIALS**
www.afm-journal.de

nanoclays such as organo MMT, halloysite, and sepiolite have been used to improve the mechanical strength of freestanding copolymer nanocomposite films. Polymer chains intercalate easily into the galleries of organo-MMT, and polymer chains can diffuse into halloysite nanotubes as well as sepiolite channels. The high aspect ratio of halloysite and sepiolite nanoclays is also one of the reasons of good mechanical strength of the nanocomposite films.

4.2. Copolymer/Clay Fiber Meshes

Membranes/scaffolds based on fiber meshes have been extensively used in biomedical applications especially in regenerative medicine as they provide unique physicochemical characteristics and mechanical properties. Their morphology to some extent replicates that of the native extracellular matrix (ECM), which is prolific to faster tissue regeneration. Scaffolds act as temporary supports at degenerated tissues and assist to regenerate tissue vastly by supplementing the structural environment for cells.[110] Hence, mimicking scaffold composition, morphology, rate of degradation and strength according to the native tissues are key factors during fabrication.[111] The clay reinforcement in such polymeric scaffolds/membranes provides an additional benefit in terms of mechanical support, thermal stability, reduced degradation time, and improved processability. Additionally, clay reinforced copolymer scaffolds can be stimuli-responsive, too.[112] Electrospinning can be used to fabricate fiber mesh-based polymer nanocomposites and varied fiber diameter and shapes including co-axial ones.[113] The electrospinning setup comprises four major parts: 1) High voltage supply, 2) Syringe pump controlling the flow rate of the copolymer/clay solution, 3) Needle spinneret charging the copolymer/clay solution, and 4) Platform to collect the fibers. The final fiber morphology of the membrane/scaffold depends on various constraints such as the applied voltage, working distance between collector and the needle tip and geometry/diameter of the needle.[114] Electrospinning has been used essentially for the fabrication of biomedical products such as scaffolds, membranes, wound dressing/drug delivery patches, and cell filtration meshes, etc. Various reports for the fabrication of copolymer-clay scaffolds/membranes and their key features are compiled in **Table 4**.[65,111,115] Wang et al.[60] demonstrated drug laponite nanodisk electrospun nanocomposite scaffolds using poly(lactic-*co*-glycolic acid) copolymer with embedded amoxicillin. The nanocomposite scaffolds showed good drug loading efficiency, sustained drug release characteristics, and antimicrobial properties without compromising their cell compatibility. In general, a higher drug loading efficiency can be achieved if the physical interaction between drug and fibrous scaffold is optimized tailoring the average pore size of the electrospun scaffold according to the size of the desired drug. Thus, it is important to optimize the spinning parameters to obtain a preferred fiber diameter in case of drug delivery applications. With poly(lactic-*co*-glycolic acid) copolymer, other clay fillers and drugs such as tetracycline hydrochloride loaded halloysite nanotube-based scaffolds have been studied by Qi et al.[67,74a] The fabricated nanocomposite scaffolds showed excellent mechanical properties, cell compatibility, antimicrobial activity,

and sustained drug release up to 42 days. MgAl-based layered double hydroxide reinforced poly(lactic-*co*-glycolic acid) nanocomposite scaffolds were used for the controlled release of flurbiprofen axetil by Yang et al.[116] Amoxicillin based antibiotics embedded in halloysite reinforced poly(lactic-*co*-glycolic acid)/chitosan blends were prepared for the fabrication of microbial protected patches for skin tissue engineering application by Tohidi et al.[117]

Multifunctional properties of nanoclays incorporated in electrospun scaffolds supported the differentiation of human mesenchymal stem cells (hMSCs) into various lineages including osteogenic, chondrogenic, myogenic, adipogenic, and neurogenic ones.[118] Poly(lactic-*co*-glycolic acid)/laponite scaffolds have been used as substrate to support osteoblast differentiation of hMSCs in osteogenic culture media[119] for bone tissue regeneration applications. Osteocalcin secretion, alkaline phosphatase (ALP) activity, and calcium deposition were marginally increased at day 14 and 21 in case of the nanocomposite scaffold as laponite has Mg and Si ions. Robust osteoblastic differentiation of hMSCs on attapulgite nanorod/poly(lactic-*co*-glycolic acid) electrospun nanocomposite scaffolds without any growth factors like dexamethasone was reported by Wang et al.[74b] Montmorillonite[9b] and laponite[120] (up to 10 wt%) were also utilized to improve the mechanical strength, hydrophilicity, cell viability, mineralization and biodegradation ability of electrospun silk fibrous membranes of silkworm silk (*B. mori*) for bone tissue engineering applications.[9b,120] Poly(glycerol-*co*-sebacate)/laponite scaffolds were prepared by salt leaching for improving ALP activity, mechanically durability, osteogenesis, in vivo biocompatibility as well as biodegradability and mineral deposition for potential bone repair applications.[115c] Interestingly, fibrous structures in combination with high aspect ratio nanoclays such as halloysite and sepiolite have been used more regularly for the preparation of scaffolds or membranes. This is because these nanoclays tend to orient along the fiber direction during the spinning process. The nanoclay orientation along the fiber axis is improving the uniaxial tensile strength, and modulus of the scaffold.

4.3. Copolymer/Clay Hydrogels

Hydrogels are polymeric morphologies that allow to resemble several shapes, they are very soft in nature and self-recoverable.[126] They can be used in biosensors, implants, scaffolds, and drug depots.[127] However, the low mechanical strength of the hydrogels does not allow distinct biomedical applications, for example, as scaffolds for tissue regeneration in load-bearing tissues and as sealants that require prominent strength as well as elongation.[128] The introduction of physical crosslinking systems such as hydrophobic interactions, supramolecular interactions, host–guest interactions, and intermolecular hydrogen bonding, etc. can considerably improve the mechanical strength of a hydrogel. Such physically crosslinked networks may break, but they reform quickly. To dissipate the energy, several strategies have been developed such as sliding-ring gels, dual-network gels like interpenetrating polymer networks (IPN), incorporating macromolecular microspheres, and hydrophobic constituents.[129] Recently, layered silicates have

Table 4. Clay/copolymer fiber meshes and their biomedical applications.

Polymer	Clay type/technique used for the preparation of scaffold/membrane	Features	Cell line and cytotoxicity evaluation (as far as available)	Application
Poly (methyl methacrylate-co-methacrylic acid)[73]	Montmorillonite and fluorohectorite/electrospinning	The spinning characteristics of the copolymer solutions were enhanced upon addition of clay nanoparticles upon increase of the viscosity, and the modulus increased. MMT clay particles were exfoliated and oriented along the fiber axis during spinning. The nanocomposite fiber showed reduced flammability as well as enhanced self-extinguishing properties.	–	Tissue regeneration and drug delivery
Poly(lactic-co-glycolic acid)[121]	Halloysite (HNT) nanotubes/electrospinning	HNT improved the tensile strength and modulus of the electrospun mat. The % cell viability was slightly reduced on clay-reinforced mats compared to that on control copolymer mats.	Mouse fibroblasts	Muscle tissue regeneration and drug delivery
Poly(lactic-co-glycolic acid)[60]	Drug loaded laponite disk/electrospinning	Amoxicillin encapsulated within laponite disks and incorporation into copolymer solutions did not affect the spinning ability, fiber diameter, and morphology. A sustained release profile was obtained, and the fabricated nanocomposite mat showed a significant zone of inhibition for bacteria.	Porcine iliac endothelial cells (PIEC), cell viability was increased ½-fold in comparison to that on control copolymers	Tissue regeneration and drug delivery
Silk fibroin from *Bombyx mori*[120]	Laponite disk/electrospinning	Mechanical properties including toughness, tensile strength as well as elastic modulus were considerably increased upon the incorporation of 5 wt% of laponite into silk fibroin matrix. Hydrophilicity, % swelling, and biodegradation were increased for the nanocomposite mats. Improved biocompatibility and pronounced (induced) apatite formation were observed for the nanocomposite membranes.	Mesenchymal stem cell proliferation was increased to 280% compared to that on silk fibroin mats	Bone regeneration
Poly(lactic-co-glycolic acid)[67]	Halloysite (HNT) nanotubes/electrospinning	Improved mechanical properties and sustained drug (tetracycline hydrochloride) release were observed for the drug-loaded HNT nanocomposite fibrous mats. There was no appreciable increase in % cell viability of the nanocomposite mats compared to control PLGA mats.	Rat fibroblasts viability was increased by 1½-fold in comparison to incubation on control copolymer scaffolds	Muscle regeneration
Poly(lactic-co-glycolic acid)[119]	Laponite disk/electrospinning	Better mechanical durability, hydrophilicity, protein adsorption capacity, cell adhesion, a slight increase in the rate of proliferation, and almost no change in hemocompatibility were observed for the prepared nanocomposite scaffolds in comparison to pristine copolymer. The nanocomposite scaffold also endorsed osteoblast differentiation of stem cells without incorporation of any growth factors.	Human mesenchymal stem cells, L929 mouse fibroblasts and porcine iliac artery endothelial cells. There was no significant cell viability difference between control copolymer scaffolds and nanocomposites	Bone regeneration
Poly(lactic-co-glycolic acid)[74b]	Attapulgite nanorod/electrospinning	Attapulgite nanorod doping did not alter the fiber morphology and hemocompatibility of the nanocomposite mat. However, biocompatibility, tensile strength, modulus, and surface hydrophilicity of the nanocomposite scaffolds were improved upon the addition of attapulgite nanorods. Stem cells differentiated into osteoblasts without any growth factors. Alkaline phosphatase activity, osteocalcin secretion, and mineralization capabilities were superior for the nanocomposite scaffolds compared to that of pristine copolymer PLGA.	Human mesenchymal stem cells, cell viability was ¼-fold increase in comparison to control copolymer scaffolds	Bone tissue regeneration
Polyurethane from poly (tetra-methylene oxide)[122]	Organically modified Montmorillonite clay/electrospinning	The exfoliated morphology was acquired for the organo clay dispersed in a PU matrix, and the d-spacing was increased compared to that of pristine MMT clay. Mechanical strength and % elasticity of the nanocomposite mats were increased compared to that of control polyurethane mats.	–	Hard tissue engineering
Silk fibroin from *Bombyx mori*[9b]	Montmorillonite clay/electrospinning	The successful nanosheet formation was achieved on the surface of pristine silk fibrous mats upon dipping the electrospun fibers into a MMT suspension yielding a thickness of 1.2 nm.	–	Tissue engineering
Poly(lactic-co-glycolic acid) with lactic acid/glycolic acid ratio of 50:50[123]	Halloysite nanotube/electrospinning	Mechanical properties like tensile strength were increased without compromising the % elongation as the HNT tubes aligned along the fibrous axis. Thermal degradation of the copolymer was decreased upon the addition of HNT tubes. Protein adsorption, cell viability, and rate of proliferation were significantly increased for the nanocomposite scaffold.	Mouse fibroblasts (L929), cell viability was slightly increased in comparison to incubation on control copolymer blend scaffolds	Muscle tissue regeneration

ADVANCED
SCIENCE NEWS
www.advancedsciencenews.com

ADVANCED
FUNCTIONAL
MATERIALS
www.afm-journal.de

Table 4. Continued.

Polymer	Clay type/technique used for the preparation of scaffold/membrane	Features	Cell line and cytotoxicity evaluation (as far as available)	Application
Poly(maleic anhydride-alt-1-octadecene)-graft-poly(L-lactic acid)[124]	Organo MMT using octadecyl amine, silver doped MMT/electrospinning	The clay incorporation formed a nano assembly within the fibrous mat. Both organo clays enhanced the thermal and mechanical properties of the nanocomposite mat.	–	Tissue engineering
Poly(lactide-co-glycolide) and poly(vinyl alcohol) blends (90:10)[115d]	Organically modified montmorillonite using quaternary ammonium salt/electrospinning	Organically modified MMT improved the degree of exfoliation in the copolymer scaffold, which led to improved tensile modulus and strength, but the % elongation was reduced significantly. The improved hydrophilicity of the nanocomposite scaffold facilitated to enhance the rate of stem cell proliferation.	Human cord blood, termed unrestricted somatic stem cells, % cell viability was increased by 33% in comparison to that on control copolymer blend scaffolds	Bone tissue engineering
Poly(lactic-co-glycolic acid)/chitosan[117]	Halloysite nanotubes/PLGA, drug (amoxicillin) and chitosan polymer/co-electrospinning	Sustained drug release characteristics were observed for the composite fibrous membranes. Addition of HNT and chitosan moieties yielded microbial protection, improved phosphate absorption as well as mechanical durability without changing the fiber morphology.	Mouse fibroblasts (L929), cell viability was unchanged	Wound dressing
Poly(lactic-co-glycolic acid)[125]	Halloysite nanotube (HNT)/electrospinning	Doping with HNTs improved the mechanical strength without diminishing the % elasticity; the blood compatibility was improved as well.	–	Tissue engineering

been incorporated into hydrogels to enhance their mechanical strength, recoverability, and biological cues by providing physical crosslinking, which is beneficial for the scaffolds, drug carrier or any kind of biosubstrates. Clay/copolymer nanocomposite hydrogels can be activated as well as controlled by various external stimuli including temperature, pH, magnetic fields, light, and electric fields for targeted drug delivery.[130] A summary of clay/copolymer nanocomposite hydrogels for various applications in drug delivery and tissue engineering are summarized in **Tables 5** and **6**, respectively.

Smart or intelligent hydrogels are interesting candidates for biomedical applications, as their properties can be triggered using external stimuli such as pH, temperature, magnetic/electric fields, and light. The responsiveness of nanocomposite hydrogels is more vital due to existence of multifunctional characteristics of nanoclays. Significant contributions have been made concerning stimuli-responsive hydrogels based on nanoclay-incorporated copolymers.[76,132,154,158] Yao et al.[76] reported on fabrication of self-assembled thermoresponsive nanocomposite hydrogels based on poly(N-isopropylacrylamide-co-acrylamide)/laponite. The prepared nanocomposite bilayer hydrogels exhibited a high extent of elongation and temperature-responsive swelling/deswelling characteristics even after many repeating cycles. Hydrogels were capable to change their shapes (rapidly, reversibly, and repeatedly) upon switching the temperature up and down. **Figure 6**a shows the strip bending upon increasing the temperature from 24 to 42 °C and its unfolding while switching the temperature again down to 24 °C. Likewise, MMT loaded poly (N-isopropylacrylamide-co-N-[3-(dimethylamino)-propyl] methacrylamide) hydrogels were reported to have excellent stimuli responsiveness.[133] The prepared bilayer nanocomposite hydrogels showed reversible as well as repeatable curling/uncurling shapes to hold any objects upon changing the pH/temperature. Figure 6b shows the curling/uncurling behavior of the fabricated hydrogels to grasp or release desired objects upon pH and temperature changes. At pH 2, it acquired 23 min to bend the strip into a circle and grasp the ring object. At pH 12, the strip released the object after 64 min. The same shape morphing behavior was applicable when changing the temperature from 60 °C (grasping) to 22 °C (releasing). Another report discussed the relationship between optical transparency and temperature switches of clay/copolymer hydrogels. The transparency of the nanocomposite hydrogels made of laponite reinforced poly (N,N-diethylacrylamide)-co-(2-dimethylamino) ethyl methacrylate was changed into slightly opaque when increasing the temperature from 20 to 40 °C (Figure 6c).[143] This outcome was due to laponite nanoclay effects on the lower critical solution temperature (LCST) of the copolymer through better reinforcement.

There have been other smart/stimuli-responsive nanocomposite hydrogels based on various copolymer/clay combinations such as oligo(ethylene glycol)/laponite,[131] 2-(2-methoxyethoxy) ethyl methacrylate/fibrillar attapulgite,[132] laponite incorporated keratin/pluronic/chitosan blends,[152] poly (2-methoxyethylacrylate-co-N,N-dimethylacrylamide)/laponite,[118a,154] poly(ethylene glycol)-b-poly(D,L-lactide-co-glycolide)/laponite,[142] poly(2-methoxyethyl acrylate)-co-(N,N-dimethylacrylamide)/laponite,[154] and poly (acrylamide-co-sodium acrylate)/laponite.[77]

Table 5. Clay/copolymer hydrogels and their application in drug delivery.

Polymer	Clay type/technique used for the preparation of hydrogel	Features	Cell line and cytotoxicity evaluation (as far as available)	Application
Chemically synthesized poly(acrylic acid-co-N-isopropyl acrylamide)[75]	Hydrotalcite clay/in situ method	Drug release performance of the nanocomposite hydrogels relayed on the surface charge of the drug molecules and quantity of the intercalated clay.	–	Drug delivery
Tailor-made thermosensitive poly 2-(2-methoxyethoxy) ethyl methacrylate-co-oligo(ethylene glycol) methacrylate[131]	Laponite clay/in situ free-radical polymerization	The exfoliated laponite clay nanocomposite morphology of the hydrogel influenced the swelling/deswelling characteristics. The prepared nanocomposite hydrogels were thermosensitive.	–	Drug delivery
Poly (2-(2-methoxyethoxy) ethyl methacrylate-co-oligo (ethylene glycol) methacrylate-co-acrylic acid)[132]	Fibrillar attpulgite (AT) clay/in situ free-radical polymerization	Tensile strength, elastic modulus as well as storage modulus were increased marginally with the incorporation of AT nanoclay. Also, T_g of the hydrogel increased, confirming the strong affinity between AT and the copolymer. The clay nanocomposite hydrogels showed stimuli-responsive behavior.	–	Drug delivery
Poly(N-isopropylacrylamide-co-acrylamide)[76]	Laponite clay/in situ free-radical polymerization	The assembled hydrogels displayed good mechanical strength without sacrificing the % elongation and swelling/deswelling characteristics owing to the formation of intermolecular hydrogen bond at the interface. The developed strategy for the assembled hydrogels enhanced the stimuli responsiveness.	–	Soft robotics and actuators
Poly (N-isopropylacrylamide and N-[3-(dimethylamino)propyl] methacrylamide][133]	MMT clay/in situ free-radical copolymerization	The developed nanocomposite hydrogel bilayers showed pH and temperature-responsive, capable of creating a robust interfacial bonding and adhered spontaneously. Tensile strength of the hydrogels improved upon addition of clay, the hydrogel shape was reversible, able to curl/uncurl upon pH, and temperature changes. These stimuli allowed the bilayer hydrogels to grasp, release, lift, and let down desired parts.	–	Soft robotics, manipulators, sensors, and drug-delivery vehicles
Poly(N,N-dimethylaminoethyl methacrylate-co-2-acrylamido-2-methyl-propanosulfonic acid)[134]	Laponite clay/in situ free-radical copolymerization	Elastic moduli increased and swelling ratio decreased upon nanoclay incorporation, as the degree of crosslinking increased for the nanocomposite hydrogel. The swelling ratio was dependent on ion composition and temperature.	–	Drug delivery
Carboxymethyl cellulose-graft-poly(acrylic acid)[135]	Organophilic MMT-nanoclay using cetyl-trimethylammonium bromide/radical graft polymerization	Organically modified clay nanocomposite hydrogels showed partially exfoliated and intercalated structure. The storage modulus (G') of the hydrogel increased marginally with increasing the OMMT content. The drug release profile was dependent on pH and crosslinking density.	–	Drug delivery
Hydroxypropyl methylcellulose-g-poly(acrylamide)[136]	Laponite clay/in situ graft polymerization	Iron nanoparticles were synthesized using laponite linked copolymers as a surfactant. The drug release profile of the magnetic hydrogel was pH-sensitive and dependent on the magnetic field.	–	Drug delivery
Gelatin[137]	Laponite clay/solution blending	The storage modulus increased significantly for the nanocomposite hydrogel due to existence of monovalent and divalent ions from laponite. However, phase separation of the hydrogel occurred for higher wt% loading of laponite and led to a deterioration of recovery of the hydrogels.	–	Drug delivery

Table 5. Continued.

Polymer	Clay type/technique used for the preparation of hydrogel	Features	Cell line and cytotoxicity evaluation (as far as available)	Application
Poly(2-methoxyethylacrylate-co-N,N-dimethylacryl-amide)[138]	Laponite clay/in situ free-radical copolymerization	Tensile strength and modulus of the hydrogels enhanced upon nanoclay addition without losing optical transparency. The transparency and swelling characteristics were relayed on temperature and salt concentration. Drug release (lidocaine and glycerin) characteristics were controlled by temperature.	–	Drug delivery
Poly(acrylic acid-co-poly(ethylene glycol) methyl ether acrylate)[139]	2-acryloylamido-2-methyl propane sulfonic acid modified hydrotalcite/in situ copolymerization	Organic modification facilitated the degree of intercalation and exfoliation of nanoclay in the hydrogels. However, the gel strength, crosslink density, and adhesive force of the hydrogel were decreased with increasing the clay content as the copolymer become more hydrophilic. Drug (vitamin B2) release characteristics dependend on network densities, electrostatic attractions, and chosen drug molecule as well as % swelling.	–	Drug delivery
Poly(acrylamide-co-sodium acrylate)[77]	Laponite clay/in situ copolymerization	The clay dispersion in nanocomposite gels showed a completely exfoliated structure. Nanocomposite hydrogels were sensitive to pH, and the % swelling ratio was directly proportional to pH.	–	Drug delivery
Gelatin-graft-poly(acrylic acid-co-acrylamide)[140]	Montmorillonite clay/in situ graft copolymerization	The nanocomposite hydrogel displayed pH-responsive drug release, high swelling ratio and improved biodegradability due to an exfoliated clay dispersion.	Human Caucasian colon adenocarcinoma- Caco-2 cell line, cell viability was drastically reduced on the nanocomposite hydrogel in comparison to that on graft copolymer hydrogels	Drug delivery
Carboxymethyl cellulose-graft-poly(acrylic acid)[141]	Layered Double Hydroxide/in situ graft polymerization	Nanocomposite hydrogels exhibited good thermal stability and high swelling ratio. Swelling ratio and drug release characteristics were sensitive to pH and temperature.	–	Drug delivery
Poly(ethylene glycol)-b-poly(D,L-lactide-co-glycolide)[142]	Laponite clay/solution mixing	The gelation rate was enriched at a very low concentration of laponite (0.75%). The storage modulus and loss modulus were enhanced significantly compared to a control copolymer hydrogel, and nanocomposite hydrogels were thermo-responsive.	–	Drug delivery
Poly (N,N-diethylacrylamide-co-2-dimethylamino ethyl methacrylate)[143]	Laponite clay/in situ copolymerization	The viscosity increased significantly and compression strength of the nanocomposite hydrogel increased from 117 to 1774 kPa at 12% laponite content. The transparency of the nanocomposite hydrogels was sensitive to temperature as the nanocomposite hydrogels were thermo-responsive.	–	Drug delivery

ADVANCED
SCIENCE NEWS
www.advancedsciencenews.com

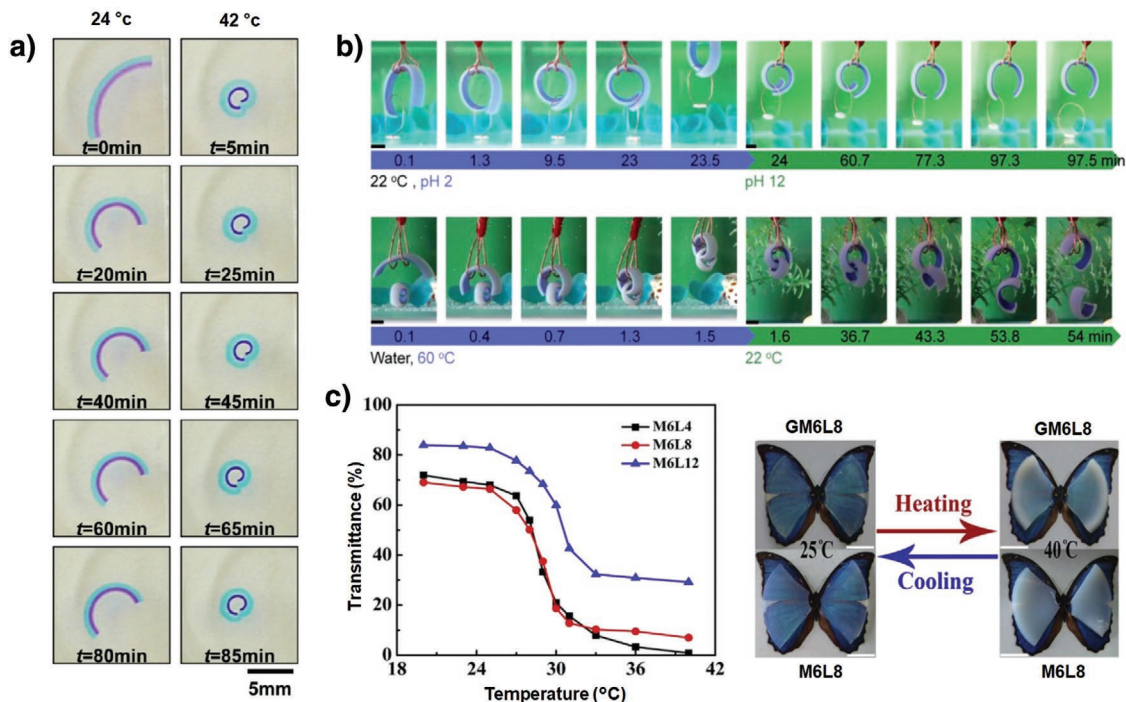ADVANCED
FUNCTIONAL
MATERIALS
www.afm-journal.de

Table 6. Clay/copolymer hydrogels and their application in tissue engineering.

Polymer	Clay type/technique used for the preparation of hydrogel	Features	Cell line and cytotoxicity evaluation (as far as available)	Application
Tailor-made isophorone diisocyanate terminated star-like poly(ethylene oxide-stat-propylene oxide)[144]	Laponite clay/solution blending method	Tensile properties of the nanocomposite hydrogels were enhanced upon addition of laponite disks. The onset degradation temperature and % char residue were also increased. The cell viability increased up to threefold.	Murine macrophages, cell proliferation was increased to 175% in comparison to that on control copolymer hydrogels	Implant coatings
Silk fibroin (RSF) of *Bombyx mori*[145]	Laponite clay/dialysis method	Robust cell proliferation and osteogenic differentiation were observed for injectable laponite nanocomposite hydrogels. Transcript levels such as alkaline phosphatase (APL) activity, osteocalcin, osteopontin, and collagen type I osteogenic markers were noticeably increased.	Primary osteoblasts from skull of newborn SD rats, fourfold increment of cell viability in comparison to that on silk fibroin hydrogels	Bone repairing
Mussel-inspired multifunctional coating from cationic antimicrobial peptide HHC-36 loaded dopamine hydrochloride grafted gelatin methacryloyl[146]	Laponite clay/solution blending method and spraying technique were used for coating	Sustained release of antimicrobial peptides from the hydrogels inhibited biofilm formation; spraying and coating of the materials demonstrated good antimicrobial characteristics. Lap shear strength of the coating enhanced upon addition of laponite. Laponite nanocomposite hydrogel augmented cell adhesion, spreading, proliferation, osteogenic differentiation, and ECM mineralization.	Human mesenchymal stem cells, % cell viability was above 90%	Implant coating for bone tissue engineering
Thiol-modified hyaluronic acid, 8-arm PEG acrylate and alginate[147]	Laponite, montmorillonite and sumecton clay/solution blending method	An excellent adhesion property to bone explants substrate was achieved leading to better osteointegration. Improved pullout strength, 36-fold increase in alkaline phosphate (ALP) activity and 11-fold increment for biomineralization were obtained for the nanocomposite hydrogels.	Human bone marrow derived mesenchymal stem cells, cell viability was 70%	Bone repairing
Mussel-inspired adhesive poly dopamine-clay-polyacrylamide[148]	Laponite clay/in situ free-radical polymerization	The prepared nanocomposite hydrogels displayed high adhesive strength, and stretchability. The gels spontaneously adhered on/stripped repeatedly (multiple cycles) from substrates without losing the adhesion property. The hydrogels showed favorable cell adhesion and proliferation and full-thickness skin wound regeneration.	NIH-3T3 fibroblasts	Skin tissue regeneration
Double strand DNA[62]	Laponite clay/solution approach	Self-healing, shear-thinning behavior and rapid self-healing ability of the clay reinforced injectable hydrogels increased the thermal stability, elasticity and allowed to maintain the structural integrity. Nanocomposite hydrogels showed a controlled release of osteogenic drug dexamethasone. The nanocomposite also demonstrated good cell viability as well as osteogenic differentiation. In vivo results from rats with cranial defects revealed a large amount of new bone formation and regeneration properties of the nanocomposite hydrogel.	Human adipose-derived stem cells, the presence of nanoclay significantly improved the cell viability	Bone regeneration
Dopamine grafted four-armed poly(ethylene glycol)[149]	Laponite clay/solution approach	Mussel inspired injectable laponite (2 wt%) reinforced nanocomposite hydrogels showed an increased rate of gelation and shear strength without losing the adhesion properties. The biodegradation rate remained the same upon addition of laponite, and minimal inflammatory response was received upon the subcutaneous implantation in the rat model.	L929 mouse fibroblasts, cell viability was above 70%	Wound dressing
Gelatin methacrylate[150]	Laponite clay/solution approach	Improved cardiac regeneration upon implanting secretome-loaded nanocomposite hydrogels into the damaged myocardium of rats. The clay greatly helped in keeping the secretome of hMSC spheroids and enhanced the biocompatibility of the gels.	Human bone marrow derived mesenchymal stem cells and Human umbilical vein endothelial (HUVEC) cells, ½-fold increment of viability was observed for the HUVEC cells in comparison to that on the control copolymer hydrogels	Cardiac tissue repair and regeneration

1908101 (17 of 28)

Table 6. Continued.

Polymer	Clay type/technique used for the preparation of hydrogel	Features	Cell line and cytotoxicity evaluation (as far as available)	Application
Poly(acrylamide-co-N,N-dimethyl aminoethyl methacrylate)[151]	Laponite clay/in situ copolymerization	The % laponite clay content controlled the crosslink density and mechanical strength. The rate of thermal degradation of the nanocomposite hydrogels was increased upon increasing the clay content.	–	Biosensors
Gelatin methacryloyl[118b]	Laponite clay/solution blending	Laponite incorporation significantly augmented cell proliferation as well as osteogenic differentiation of stem cells. Improved in vivo biocompatibility and minimum localized immune response were observed for the nanocomposite hydrogels.	Bone marrow derived human mesenchymal stem cells	Bone regeneration
Wool-derived fibrous protein (keratin) and Pluronic grafted chitosan[152]	Laponite clay/graft copolymerization	Gelation rate, swelling ratio, thermo-responsiveness, and storage modulus were considerably improved for the nanocomposite hydrogels. They also showed excellent biocompatibility, cell adhesion and proliferation.	Articular chondrocytes isolated from rabbits knee joints, cell viability was above 90%	Articular cartilage tissue engineering
Sodium alginate[153]	Laponite clay/solution blending	Compression strength enhanced upon addition of laponite without harming the injectability. Thermal stability slightly decreased for the nanocomposite hydrogels.	MG63 osteoblasts, cell viability was threefold increased in comparison to control copolymer hydrogels	Bone tissue engineering
Alginate acid sodium salt and doxorubicin hydrochloride (Dox)[61]	Laponite clay/solution blending	Nanocomposite hydrogels presented good gel stability, sustained release characteristics (up to 17 days), improved antitumor efficiency, and controlled degradation.	Cellosaurus cell line CAL-72 (osteosarcoma cell line), slight reduction of cell viability was observed	Cancer therapy
Collagen type I[68]	Laponite clay/solution blending	No improvement in mechanical strength of the hydrogels upon incorporation of nanoclay. However, the sprout network formation (endothelialization) was better for the nanocomposite hydrogels.	Human umbilical vein endothelial cells	Proangiogenic therapeutics
Poly(2-acrylamido-2-methyl-propane sulfonic acid-co-acrylic acid-co-sodium acrylate)[68]	Organically modified bentonite clay using a cationic surfactant (3-methacrylamidopropyl) trimethyl ammonium chloride/in situ solution polymerization	Organic modification of nanoclay decreased the swelling of the nanocomposite hydrogels and enhanced the network density. Mechanical properties including static and dynamic strength of the hydrogels were increased with increasing clay content.	–	Bone tissue engineering
Poly (2-methoxyethyl acrylate-co-N,N-dimethylacrylamide)[118a]	Laponite clay/in situ copolymerization	Swelling behavior of nanocomposite hydrogels was temperature responsive. Protein adsorption (immunoglobulin), cell attachment as well as the proliferation of various cells lines were enhanced upon the addition of nanoclay.	Human mesenchymal stem cells, neonatal human dermal fibroblasts and human osteosarcoma cells	Bone regeneration
Poly(2-methoxyethyl acrylate-co-N,N-dimethylacrylamide)[154]	Hectorite clay/in situ free-radical copolymerization	Stimuli-response upon a change in temperature, ion concentration, pH and solvent. Nanocomposite hydrogels demonstrated excellent tensile strength, high elongation (more than 1000%) without suppressing the transparency.	V79 from Chinese hamster lung fibroblast cell line, cell viability was reduced upon addition of the nanoclay	Skin tissue engineering
Gelatin (type-A)[155]	Laponite clay/solution mixing	Shear-thinning characteristics, gel stability, injectability, cell compatibility, and blood coagulation (in vitro as well as in vivo) were improved upon reinforcement of laponite. Also, the nanocomposite hydrogels did not show any immune response upon subcutaneous implantation in the rat model.	Mouse monocyte/macrophage RAW 264.7 cells, cell viability was above 85%	Wound repairing
Poly(trimethylene carbonate)-b-poly(ethylene glycol)-b-poly(trimethylene carbonate)[156]	Laponite clay/solution mixing	The toughness of the hydrogels increased from 25 to 200 kJ m^3 and the compressive modulus increased from 15 to 67 kPa upon clay incorporation. The nanocomposite was degradable in the presence of cholesterol esterase. Macrophage adhesion was promoted with increasing the clay content.	Murine macrophages	Tissue engineering and drug delivery
Poly(acrylic acid-co-methylene bisacrylamide)[157]	Polyacrylamide-modified kaolinite/in situ copolymerization	Organic modification improved the polymer-filler interaction, which enabled the hydrogels to increase their swelling ability, porosity, and storage modulus.	–	Implants

1908101 (18 of 28)

**ADVANCED
SCIENCE NEWS**
www.advancedsciencenews.com
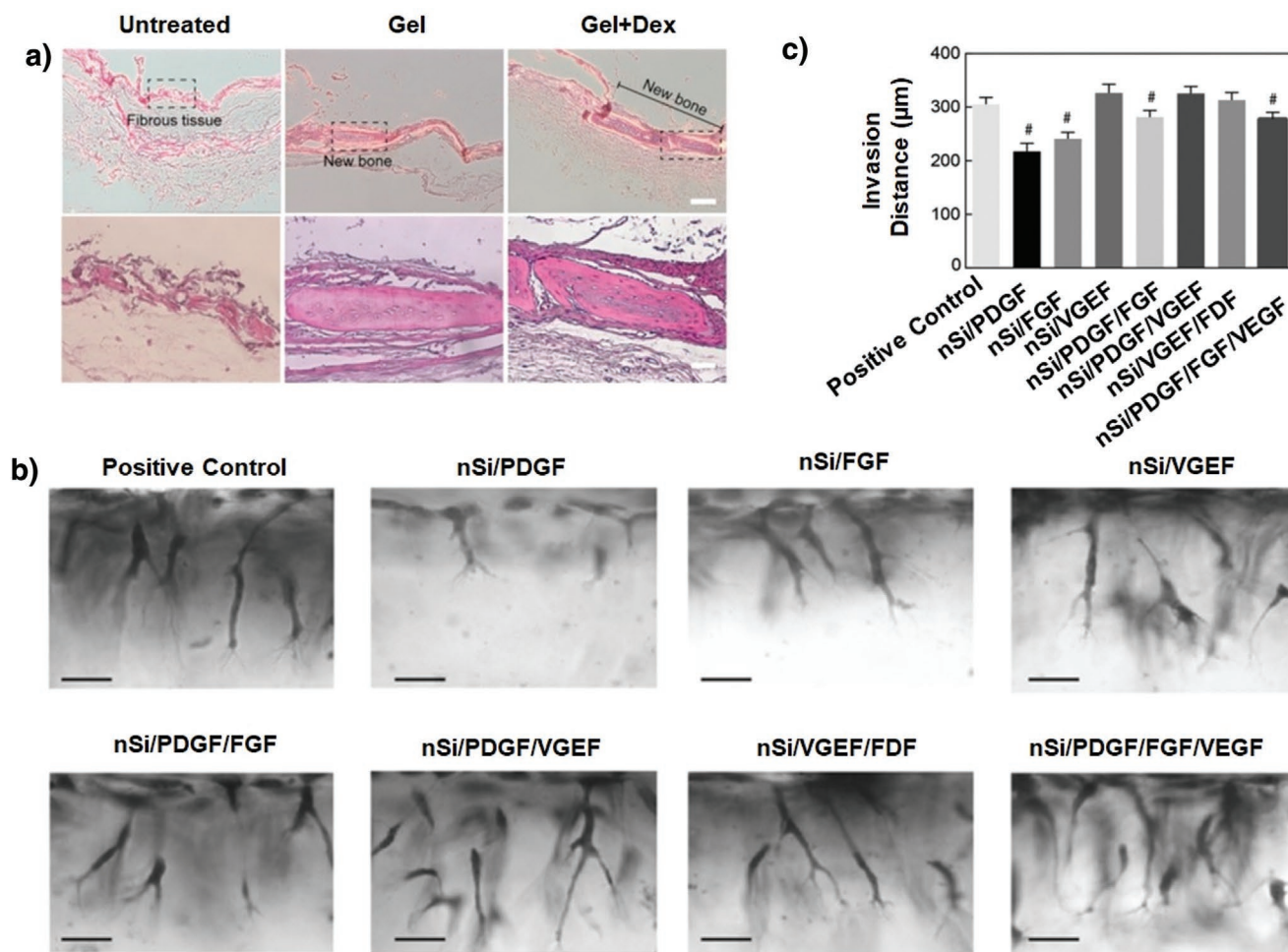
**ADVANCED
FUNCTIONAL
MATERIALS**
www.afm-journal.de

Figure 6. a) Repeatable thermoresponsive behavior of bilayer poly(*N*-isopropyl acrylamide-*co*-acrylamide)/laponite hydrogel strips in water at different time points and temperature, b) Grasping and releasing the ring objects upon pH and temperature stimulus of MMT reinforced poly(*N*-isopropylacrylamide-*co*-*N*-[3-(dimethylamino)-propyl] methacrylamide) copolymer hydrogel bilayer strips. c) Changes of optical characteristics upon heating and cooling of laponite incorporated poly(*N*,*N*-diethylacrylamide)-*co*-(2-dimethylamino) ethyl methacrylate copolymer hydrogels in the shape of a butterfly. a) Reproduced with permission.[76] Copyright 2016, ACS. b) Reproduced with permission.[133] Copyright 2018, ACS. c) Reproduced with permission.[143] Copyright 2017, Elsevier.

The responsive behavior of the copolymer/clay nanocomposite hydrogels is due to many factors such as phase transition temperature (LCST and UCST), inter/intra molecular hydrogen bond interaction, type of crosslinking, density and protonation–deprotonation of side/pendant groups of the polymer chains.[98,102,158] Smart hydrogels can be used in biomimetic soft robotics for vehicles, drug delivery, manipulators, and actuators.[159] On the other hand, nanocomposite hydrogels have been used in regenerative medicine as a cell/protein/drug delivery carrier, as soft implants, and scaffolds due to their exceptional physical and biological characteristics. They possess an interconnected porous structure (3D environment), self-recoverable shape and they are soft in nature, which is convenient for the patient during implantation.[160] The nanoclay incorporation can modify the mechanical strength of the copolymer hydrogels according to the tissue to be regenerated. Clays not only assist in improving the mechanical requisite of the copolymer hydrogels, but they too enhance the biological characteristics and drug release characteristics, as the clays contain minerals such as Si, Mg, Ca, and, Hasany et al.[147] demonstrated that sumecton, laponite, and montmorillonite (up to 0.5 wt%) incorporated into thiol-modified hyaluronic acid/alginate blend hydrogels can be used for bone tissue regeneration. The prepared nanocomposite hydrogels displayed excellent mechanical strength, increased hMSCs viability, promoted robust stem cell proliferation and differentiation ability compared to that of pristine thiol-modified hyaluronic acid/alginate blend hydrogels. Nanocomposite hydrogels exhibited

a 36-fold increment of ALP activity of hMSCs with increased biomineralization compared to control copolymer hydrogels. The combinatorial improvement in many properties was due to better polymer-filler affinity, additional crosslinking as well as partially intercalated/partially exfoliated morphologies of the clay/copolymer nanocomposites. Among three clays, MMT showed the best performance as it strongly interacted with the polyanionic copolymer matrix. Bioactive nanocomposite hydrogels made of GelMA/laponite with robust ALP activity showed an improved osteogenic protein synthesis and in vivo biocompatibility in the absence of any growth factors for bone regeneration purposes.[118b] DNA/laponite based injectable hydrogels were studied by Basu et al.[62] and showed improved osteogenic differentiation of stem cells, calcium deposition, long term biodegradability, sustained drug release, and a high volume of new bone formation at the cranial bone defect. However, no significant difference in cell viability or proliferation was observed between the control and the nanocomposite hydrogel even after 72 h of cell culturing.

Figure 7a displays the hematoxylin and eosin (H&E) stained sections 4 weeks after implantation of various hydrogels placed in calvarial defects in rats. The study demonstrated that the nanocomposite hydrogels showed high volume/area of new bone formation compared to the control and there was no sign of inflammation/infection. Han et al.[148] developed mussel-inspired nanocomposite hydrogels based on polydopamine/laponite disks with up to 15 wt% to be used as wound dressings. The prepared nanocomposite hydrogels exhibited

**ADVANCED
SCIENCE NEWS**

www.advancedsciencenews.com

**ADVANCED
FUNCTIONAL
MATERIALS**

www.afm-journal.de

Figure 7. a) Hematoxylin and eosin (H&E)-stained sections of nanocomposite hydrogels (dexamethasone loaded DNA/laponite) placed in a calvarial defect in rats analyzed 4 weeks after implantation (lower panel scale bar 200 μm and upper panel scale bar 50 μm) compared to untreated defects to show the new bone formation and regeneration, b) Laponite was doped with various growth factors such as vascular endothelial growth factor (VEGF), fibroblast growth factor (FGF), and platelet-derived growth factor (PDGF) and then suspended in a gradient collagen-I matrix to visualize endothelial sprouting or angiogenic responses. More endothelial sprouting was observed from the nanosilicate and VEGF combination (scale bar = 50 μm). c) Sprouting distance of endothelial cells in gradient materials doped with various growth factors were taken from the microscopic results. a) Reproduced with permission.[62] Copyright 2018, ACS. b,c) Reproduced with permission.[68] Copyright 2018, Wiley-VCH.

excellent adhesion properties on various substrates. There was no significant drop of adhesion strength even after multiple repeats using different substrates. In vitro and in vivo results depicted that the nanocomposite hydrogels showed better cell compatibility, improved rate of proliferation, and excellent full-thickness wound regeneration (after 21 days). The thick epidermis layer was evident from the histological photomicrographs. The biodegradation of the nanocomposite hydrogels was also noticed from the histopathology images. Regrettably, a minor inflammatory response was observed within the stained sections. Dopamine-modified four-armed poly(ethylene glycol) nanocomposite hydrogels reinforced with laponite disks up to 2 wt% were used for fabricating bioadhesive substrates with improved bioactivity for muscle tissue regeneration.[149] Improved blood compatibility, hemostasis, reduced clotting time, and injectability of laponite reinforced (up to 9 wt%) gelatin hydrogels (type A) from porcine skin for hemorrhage treatment were published by Gaharwar et al.[155] Howell et al.[68] used

laponite nanodisks loaded with proangiogenic proteins such as vascular endothelial growth factor (VEGF), fibroblast growth factor (FGF), and platelet-derived growth factor (PDGF) to stimulate the endothelial cell invasion in a collagen-I hydrogel gradient as a 3D in vitro model of angiogenesis. The samples with growth factors/proteins loaded nanoclays demonstrated more endothelial sprouting compared to samples without clay. Figure 7b shows sprouting of the endothelial cells inside the collagen hydrogels. Figure 7c shows the sprouting distance of endothelial cells in different gradient materials doped with various growth factors. Growth factors incorporated within laponite nanocomposites enabled more sprouting of endothelial cells network. Owing to clay structure and tunable composition, clay/copolymer hydrogels have been broadly used in drug delivery, too. Such hydrogels are capable of accommodating high amounts of drugs, restrict the initial burst release by tortuous diffusion as well as favorable nanoclay-drug interactions, and allow pH/temperature regulated drug release at the desired

ADVANCED
SCIENCE NEWS
www.advancedsciencenews.com

ADVANCED
FUNCTIONAL
MATERIALS
www.afm-journal.de

place/tissue and long-term delivery. Copolymer/clay nanocomposite hydrogels such as poly(acrylic acid-co-N-isopropyl acrylamide)/hydrotalcite with caffeine as a model drug,[75] doxorubicin embedded laponite/alginate for cancer therapy,[61] hydrotalcite reinforced poly[acrylic acid-co-poly(ethylene glycol) methyl ether acrylate] for vitamin B$_2$ release,[139] gelatin-graft-poly(acrylic acid-co-acrylamide)/montmorillonite for vitamin B$_{12}$ release along with improved blood compatibility[140] and carboxymethyl cellulose-g-poly(acrylic acid)/Mg, Al-layered double hydroxide for the controlled release of vitamin B$_{12}$ have been used as drug carrier for therapies in various fluid conditions such as artificial gastric fluids (AGF) and in artificial intestinal fluid.[141]

4.4. Copolymer/Clay Nanocomposites Processed Using 3D Printing

New biomaterials are needed for regenerating large segmental tissue degeneration resulting from trauma, tumor resections or inflammation.[161] In regenerative medicine, the prime objective is to fabricate constructs mimicking native tissues in terms of composition, mechanical durability and architecture for better healing efficiencies. 3D printed constructs can facilitate robust cell migration, good rates of proliferation and differentiation and enhanced angiogenesis or vascularization.[162] Biofabrication or 3D printing is an emerging technology, which has the capability of generating tissue-analog structures or constructing 3D scaffolds with more than two types of cells within a suitable matrix including core–shell hollow tubes as 3D microenvironments for cells, which can bring extraordinary functional characteristics and provide all the biological cues for faster tissue regeneration.[81a,115f,163] The most common types of printing methods are inkjet, extrusion-based, and laser-assisted printing.[164] Among all, extrusion-based printing is proficient and suitable for most of the polymers as well as for nanocomposites.[165] The precise viscosity of the bioinks or hydrogels is very important especially for cell printing. A viscosity less than 300 mPa s of any hydrogel is not proficient to preserve the shape fidelity of the desired 3D construct.[166] However, higher viscosities of bioinks are not appropriate for cell printing as they require higher pressure to dispense, and eventually the embedded cells experience higher shear stress, which can damage the cells.[167] Therefore, nanomaterials within the hydrogels can alter the physicochemical properties and enhance the bioink processing characteristics (easy handling). Nanoengineered bioinks opened a range of new prospects to recover the shape of 3D printed scaffolds along with many unique properties, such as bio-mineralization, controlled drug release, mechanical strength, photoresponsiveness, rapid gelling, self-crosslinking ability, and conductivity.[168] Among various nanomaterials, nanoclays appeared to be an efficient additive for the preparation of nanoengineered bioinks.[169] They can enhance the flow behavior, shape recovery, and biological activity of bioink. Nanoclays are water dispersible and have heterogeneous charge distributions (negatively charged surfaces with positively charged edges). This allows increasing the viscosity, physical crosslinking, and mechanical strength of bioinks by ionic interactions with the nanoclays. Clay/copolymer nanocomposite bioinks show good flow behavior and shape fidelity by providing additional mechanical strength via physical crosslinking. Owing to the "house of-cards" structure of clays, the thixotropic shear-thinning flow behavior of nanocomposite bioinks is enhanced, and gels crosslink right after printing.[170] Additionally, clay nanocomposite bioinks can be stimuli-responsive toward electrical, temperature and pH stimuli.[171] The stimuli-response of cell containing 3D constructs is very useful in cardiac and skeletal muscle tissue regeneration, as myoblasts are more proactive, proliferate faster and show a more efficient differentiation into myotubes upon electrical or mechanical stimulation.[172] **Table 7** summarizes the detailed information on the developed copolymer/clay nanocomposite bioinks used for biofabrication.

Agarose/laponite disk nanocomposite bioinks with improved printing characteristics allowed the production of complex shapes (multiple layers of hollow tubes and cuboids) and showed good metabolic activity and cell spreading of encapsulated HeLa and 3T3 cells.[175] An inherent ionic interaction between agarose and the clay was the reason for improved properties and biological characteristics. Constructs, such as a human ear, where 3D printed using thermo-reversible hydrogels comprising kappa-carrageenan (κCA)/inorganic polyphosphate shielded laponite.[173] The developed nanocomposite bioink provided mechanical durability, printability and yielded shape retention characteristics owing to the formation of strong intermolecular hydrogen bond interactions between the clay and kappa-carrageenan. MC3T3-E1 mouse preosteoblasts showed good viability in printed constructs as shown in **Figure 8**a. The cells were evenly distributed throughout the constructs. In another study, nanoengineered ionic-covalent entanglement (NICE) bioinks comprising laponite/gelatin methacryloyl (GelMA) blended with κCA were developed for the fabrication of mechanically stiff and elastomeric 3D biostructures such as bifurcated vessels, and a human ear with 150 layers[64] as shown in Figure 8b. Mice preosteoblast containing biostructures were flexible, showed excellent compression strength and long term cell viability with greater spreading throughout 121 days of culture compared to that of control hydrogels (without laponite). At day 30, the color of the cell printed construct transformed from translucent to slightly opaque, which showed that strong ECM deposition and favorable nutrient transport had occurred.
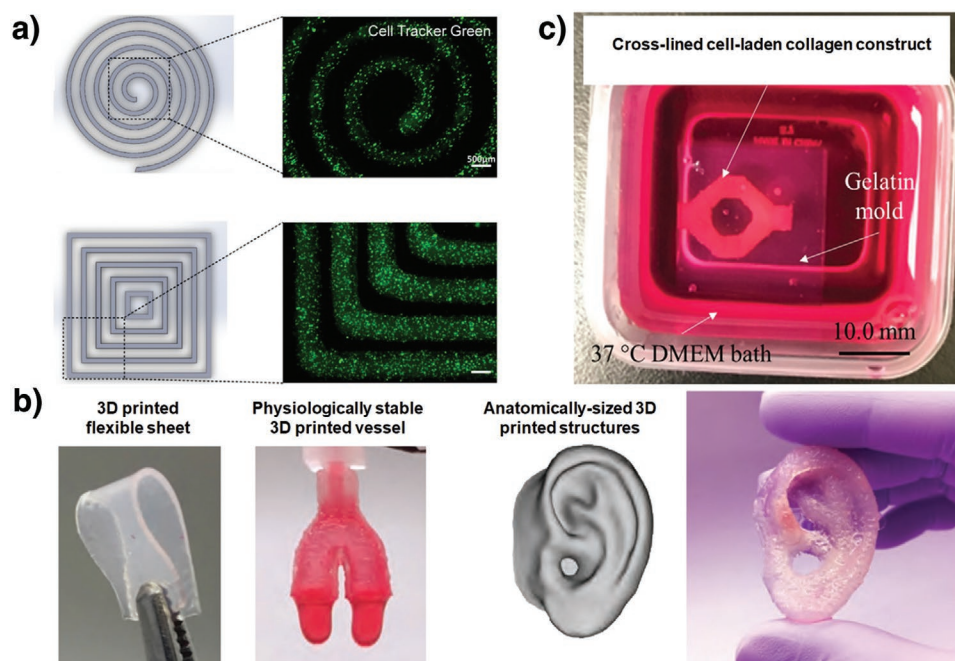
Jin et al.[65] fabricated perfusable, free-standing flexible vascular networks with annular channels from mouse fibroblast-laden sodium alginate/laponite (6 wt%) and of collagen-based fugitive bioinks using co-axial bioprinting. Fabricated cell-laden hollow vascular networks in culture media are shown in Figure 8c. Ahlfeld et al.[176] fabricated hMSC-laden laponite/alginate and methylcellulose 3D constructs with varying structures like hollow tubes with cubic shapes for the sustained release of in situ loaded proteins like bovine serum albumin and vascular endothelial growth factor for muscle tissue regeneration. The printed cells were viable over 21 days, and the shape of the constructs retained throughout the culturing period due to strong bonding between the nanoclay and the copolymer. Robust cell proliferation, osteogenic differentiation, calcium deposition and angiogenesis of the human bone marrow stem cells was shown in 3D printed GelMA hydrogel cubic constructs.[177] A chick

Table 7. Clay/copolymer-based inks used for 3D printing and their biomedical applications.

Bioink	Clay types/type of printer used for the fabrication of 3D construct	Features	Cell line and cytotoxicity evaluation (as far as available)	Application
Alginate and carboxy-methyl cellulose[166]	MMT/Extrusion based printing	The addition of clay minerals (MMT) improved the shape fidelity of the 3D constructs by a higher crosslinking density, which enabled to print various complex shapes and patterns like cuboids and tubes.	Human pancreatic cancer cells, 94% cell viability	Tissue engineering
Poly(ethylene glycol) diacrylate (PEGDA)[63]	Laponite nanodisk/extrusion based printing	Addition of laponite increased the bioink viscosity and modulus and network stability by providing additional physical crosslinks. The nanocomposite bioinks had self-recovery and shear-thinning flow characteristics enabled printing of complex pattern.	Murine preosteoblasts, long-time cell viability above 96% was observed for the cell printed constructs	Muscle tissue engineering
Agarose[175]	Laponite nanodisk/extrusion based printing	Addition of laponite (3%) into agarose induced the formation of hydrogels without any crosslinking agent. The hydrogels provided good mechanical properties (modulus-G', and shear stress) and shear thinning characteristics, and showed improved shape fidelity of the fabricated complex structures including multilayer tubes. The laponite reinforcement improved the metabolic activity and spreading efficiency of cells within the printed constructs.	HeLa and NIH/3T3 cells, the cell spreading area was 50-fold increase in comparison to the control copolymer	Tissue engineering
Sodium alginate and gelatin[180]	Laponite nanodisk used as a suspension bath for curing the constructs/extrusion printing	Laponite was used to solidify 3D cell printed constructs. The concentration and pH of the laponite suspension influenced the shape recovery and mechanical properties of the printed microvascular hollow tube constructs.	NIH/3T3 fibroblasts, onefold increment of cell viability in comparison to the control copolymer blend	Vascularized tissue engineering
Poly(ethylene glycol) diacrylate (PEGDA), alginate and gelatin[115a]	Laponite nanodisk/extrusion based printing for the cup and triple-walled tubular structures	Robust cell proliferation was observed after 7 days of incubation of the cell printed cup and tubular constructs.	NIH-3T3 mouse fibroblasts, cell viability was fivefold increase compared to that of control copolymer blends	Skin tissue repair
kappa-carrageenan (κCA)[173]	Laponite nanodisk/extrusion type printing	Laponite enhanced the mechanical strength of the bioink by providing additional crosslinks. Thermoresponsive bioinks were obtained by tuning the ratio of laponite/κCA.	MC3T3-E1 mouse preosteoblasts, 90% cells were viable	Bone tissue regeneration
Gelatin methacryloyl (GelMA) with kappa-carrageenan (κCA)[64]	Laponite nanodisk/extrusion type printer	Ionic-covalent entanglement (NICE) bioinks were developed using laponite and gelatin to improve the biological characteristics and printing abilities of the printed structures like human-scale bronchus, Y-shaped blood vessel, and an ear. Cell viability was maintained for more than 120 days in these constructs.	Murine 3T3 preosteoblasts, 92% cells were viable	Bone and skin tissue regeneration
Sodium alginate and collagen-I for vascular tree type printing pattern[65]	Laponite nanodisk/extrusion based bioprinting	Laponite was used as a quencher for the printed vascular tree construct and helped improving the gelation rate, mechanical strength, and shape retention.	NIH-3T3 fibroblasts, cell viability of the cell printed constructs was 92%	Vascularization of tissue
Poly(ethylene glycol)-b-poly(propylene glycol)-b-poly(ethylene glycol) and poly (N-isopropyl acrylamide)[158]	Laponite clay/extrusion type printing	Laponite improved the printing characteristics of the hydrogels by providing additional crosslinks. Addition of spare amounts of CNT into the laponite reinforced hydrogels gained multifunctional properties like conductivity, high flexibility, self-healing features, and good adhesion characteristics. The conductivity of the 3D printed constructs made they very sensitive/responsive to heat and NIR light. Thus, they can be used as a sensor to monitor finger bending, wrist movement, elbow actions, knee bending, etc.	L929 fibroblasts, cell viability was higher than 90%	Wearable sensors

Table 7. Continued.

Bioink	Clay types/type of printer used for the fabrication of 3D construct	Features	Cell line and cytotoxicity evaluation (as far as available)	Application
Poly(acrylamide) and agarose[179]	Laponite clay/melt extrusion printing	Laponite improved the printability of the agarose/acrylamide blend as well as the shape transformation (4D) by heating and cooling the printed constructs. The bioink was successfully printed into a whale shark structure. The shark mouth opened while applying an external force and cooling. The developed bioink was also printed into an octopus-like structure and it seemed to become alive (tentacle arms and legs) upon cooling.	–	Soft robotics and microfluidic devices
Alginate and methylcellulose[176]	Laponite disk/extrusion printing	The laponite enhanced the shape fidelity of the printed tubes and cubic structures by providing desired mechanical cues. The printed constructs expressed controlled release of bovine serum albumin and vascular endothelial growth factors.	Human mesenchymal stem cells, 70–75% cells were viable	Skeletal tissue engineering
Poly(N,N′-Methylenebisacrylamide-co-acryloylbenzophenone)[181]	Laponite disk/extrusion printing	The copolymer/laponite bioinks were printed on mesostructured stimuli-responsive electrospun membranes. The total constructs (3D printed and electrospun) were capable to fold into tubes upon heating in aqueous solution. Laponite enhanced the mechanical characteristics of the bioink as well as the rate of shape morphing of the constructs.	–	Tissue engineering
Gelatin methacryloyl[177]	Laponite disk/extrusion printing	Cell viability of the printed constructs was above 85% on day 21, but in case of pristine GelMA printed constructs as low as 55%. The rate of proliferation was higher in presence of the nanocomposite bioinks, which encouraged osteogenic differentiation and vascularization (ex vivo).	Human bone marrow stromal cell, cell viability increased to 95% from 55% (control copolymer)	Skeletal tissue regeneration
Sodium alginate[182]	Laponite disk/extrusion printing	The bioink was optimal at 6 wt% laponite with improved deswelling and mechanical strength.	–	Tissue engineering
Gelatin methacrylate[174]	Laponite disk/extrusion printing	The nanocomposite bioink was successfully printed into various complex structures such as an ear, branched vessels and grid scaffolds. Incorporation of nanoclay improved the porosity, tensile strength, reduced the degradation ratio, improved the cell compatibility and the rate of proliferation	Human umbilical cord vein endothelial cells, cell proliferation was twofold increase in comparison to that incubated on the control copolymer	Tissue regeneration
Sodium alginate and polyethylene glycol diacrylate (PEGDA)[178]	Laponite disk/extrusion printing	The nanocomposite hydrogel was successfully printed into various complex structures like a hollow cube, hemisphere, pyramid, bilayer grid scaffold, twisted bundle, the shape of an ear, and a nose. Laponite improved the tension and compression modulus of the hydrogel with enhanced fracture toughness.	Bone marrow derived human mesenchymal stem cells and human embryonic kidney 293 cells, nearly, 100% cells were viable	Tissue engineering
Gelatin methacrylate[183]	Laponite disk/extrusion printing	The incorporation of laponite disks enhanced stiffness and in vitro enzymatic stability of the bioinks. Nanocomposite 3D constructs supported cell adhesion and proliferation rate and promoted osteogenic differentiation without incorporation of growth factors.	Preosteoblast cell lines and NIH MC3T3 fibroblasts, 60% cells were viable	Bone regeneration
Poly(trimethylene carbonate)-co-poly(ethylene glycol)-co-poly(trimethylene carbonate)-methacrylic anhydride[156]	Laponite disk/stereolithography	3D constructs showed maximum compression strength of 1.12 MPa, modulus of 33.6 kPa and elongation at break of 94%. The designed porous nanocomposite 3D scaffold was degraded slowly.	Macrophages	Tissue engineering
Hyaluronic acid sodium salt and polyethylene glycol diacrylate (PEGDA)[184]	Laponite disk/extrusion printing	Two adjacent channels were printed with different bioinks. 95% cell viability was observed for the printed constructs. The differentiation capability and mineralization (in vivo) was pronounced for the nanocomposite bioinks.	Primary rat osteoblasts, cell viability was onefold increased in comparison to that on control copolymer printed constructs	Bone tissue engineering

Figure 8. a) Live/dead cell assay of MC3T3-E1 mouse preosteoblasts cultured on printed laponite/kappa-carrageenan ink after 7 days (scale bars = 500 µm). b) Laponite/GelMA with kappa-carrageenan (κCA) printed into mechanically stiff and flexible 3D biostructures functioning as flexible sheets, bifurcated vessels, and providing a human ear shape. c) Perfusable, free-standing flexible vascular network with annular channels made of sodium alginate/laponite (6 wt%) and of collagen-based inks laden with mouse fibroblasts using co-axial bioprinting. a) Reproduced with permission.[173] Copyright 2017, ACS. b) Reproduced with permission.[64] Copyright 2018, ACS. c) Reproduced with permission.[65] Copyright 2018, ACS. c) Reproduced with permission.[174] Copyright 2019, IOP Publishing.

chorioallantoic membrane (CAM) assay confirmed blood vessel penetration into the hydrogels, which was more prominent for the nanocomposite hydrogels compared to that of GelMA. The GelMA/laponite bioink was fabricated into an ear-shaped construct. Live/dead cell assays of the cultured endothelial cells on the printed constructs confirmed rapid cell proliferation and cell adherence after 5 days of culture. The cells protruded into the printed strands. Laponite/sodium alginate bioinks enabled to print highly stretchable and strong/toughened complex 3D constructs with the shape of a human ear, nose, hollow cube, hemisphere, pyramid, and twisted bundle.[178] There was no significant reduction in modulus, strength, and elongation even after three cycles of compression. Nevertheless, human embryonic kidney (HEK) cells cultured on the printed constructs showed more than 75% survival rate after 5 days of culturing. Thermoresponsive shape morphing constructs in the form of an octopus and whale-like structures using laponite/ acrylamide-co-agarose bioinks were reported by Guo et al.[179] The shape of the octopus and whale deformed instantly upon heating and cooling. A comparative analysis of different clays used in copolymer nanocomposite hydrogels or bioinks for 3D cell printing for biomedical applications showed that laponite is better suitable than other clays for the preparation of stimuli-responsive hydrogel/bioinks for tissue regeneration as well as drug delivery due to its better electrical conductivity.[68] The electrical conductivity of nanoclays was also useful to align the cells in a particular direction and in promoting cell differentiation. The disk size of laponite is similar to the domain size of many block copolymers, which encourages the molecular interaction

between the copolymer and the nanoclay during hydrogel formation. Laponite bioinks also showed good mechanical stability for shape-fidelity of 3D bioprinted constructs and shape memory characteristics by providing physical crosslinking with the copolymer chains. Laponite reinforced copolymer bioinks have been capable to print free-standing cell-laden scaffolds without any crosslinker.[63]

5. Conclusions and Outlook

Copolymer/clay nanocomposites are one of the most versatile class of materials to be used in biomedical applications. In this review, we have discussed different preparation techniques of clay/copolymer nanocomposites morphologies for various biomedical applications. Due to a unique architecture, availability, and tailor-made composition of nanoclays, copolymer/ clay nanocomposites show several advantages compared to other materials. Copolymer/clay nanocomposites provide multifunctional features such as mechanical strength, chemical stability, biodegradability, barrier properties, blood compatibility, good cell interactions, allow for cell differentiation, faster tissue regeneration, induced vascularization, sustained drug releases, show shape memory effects and stimuli response. Clay incorporation into copolymer matrices also enhances their processability/flowability by augmenting physio-chemical characteristics. We have shown the potential of various copolymer/ clay nanocomposites processed into hydrogels, scaffolds/membranes, cell-laden 3D constructs and thin films for applications

**ADVANCED
SCIENCE NEWS**

www.advancedsciencenews.com

**ADVANCED
FUNCTIONAL
MATERIALS**

www.afm-journal.de

in tissue regeneration, orthopedic implants, drug delivery, and fabrication of microfluidic devices. Although several reports are available on copolymer/clay biomaterials, still there is plenty of room for further development of exfoliation or intercalation strategies for clay and its implementation into copolymer matrices. The most important challenge is the increase of the maximum quantity of clay to be incorporated into copolymer matrices, which is still favorable for cells. Wide opportunities and challenges are provided by 3D printing of copolymeric inks such as clay-reinforced nylon 12, polyurethane and other thermoplastic/vulcanized nanocomposites. Unlocking the mystery of using such copolymer inks for 3D printing will be beneficial for several applications as these polymers are frequently used in engineering. In terms of biomedical applications, modification of nanoclays using Ca^{2+} and phosphoryl moieties can be attempted, since calcium and phosphates are useful to enhance the biomineralization as well as bone regeneration. Furthermore, the unexplored status of clay minerals released from the composite after degradation of the organic compounds is an unresolved issue. In this context, analytical and imaging techniques such as advanced Raman spectroscopy, TGA/mass coupled IR spectroscopy, as well as tagging nanoclays with fluorescent dyes followed by characterization using live MRI can be utilized to localize clay minerals in cells or tissues. Advanced techniques such as genomics, metabolomics, and proteomics can also be used to get insights into the molecular pathways of the released clay minerals in body tissues. After thorough investigations of the aforementioned limitations including approval from the Food and Drug Administration (FDA), copolymer/clay nanocomposites can be an excellent advanced biomaterial and likely be used more often for biomedical applications in the future.

Conflict of Interest

The authors declare no conflict of interest.

[1] P. Podsiadlo, A. K. Kaushik, E. M. Arruda, A. M. Waas, B. S. Shim, J. D. Xu, H. Nandivada, B. G. Pumplin, J. Lahann, A. Ramamoorthy, N. A. Kotov, *Science* **2007**, *318*, 80.

[2] Y. Ke, P. Stroeve, *Polymer-Layered Silicate and Silica Nanocomposites*, Elsevier, Amsterdam **2005**.

[3] A. Blumstein, *J. Polym. Sci. Part A: Gen. Pap.* **1965**, *3*, 2653.

[4] a) M. Ito, K. Nagai, *J. Appl. Polym. Sci.* **2010**, *118*, 928; b) L. Timochenco, V. Grassi, M. Dal Pizzol, J. Costa, L. Castellares, C. Sayer, R. Machado, P. Araújo, *eXPRESS Polym. Lett.* **2010**, *4*, 500. c) X. Huang, S. Lewis, W. J. Brittain, R. A. Vaia, *Macromolecules* **2000**, *33*, 2000; d) K. Strawhecker, E. Manias, *Chem. Mater.* **2000**, *12*, 2943.

[5] a) M. A. Ahmed, U. F. Kandil, N. O. Shaker, A. I. Hashem, *J. Radiat. Res. Appl. Sci.* **2015**, *8*, 549; b) S. Barua, N. Dutta, S. Karmakar, P. Chattopadhyay, L. Aidew, A. K. Buragohain, N. Karak, *Biomed. Mater.* **2014**, *9*, 025006.

[6] a) J. Diez, R. Bellas, C. Ramirez, A. Rodriguez, *J. Appl. Polym. Sci.* **2010**, *118*, 566; b) S. S. Markanday, J. Stastna, G. Polacco, S. Filippi, I. Kazatchkov, L. Zanzotto, *J. Appl. Polym. Sci.* **2010**, *118*, 557; c) S. J. Ahmadi, H. Yudong, W. Li, *Iran Pol. J.* **2004**, *13*, 415; d) I. Ghasemi, M. Karrabi, M. Mohammadi, H. Azizi, *eXPRESS Polym. Lett.* **2010**, *4*, 62.

[7] a) A. Okada, A. Usuki, *Mater. Sci. Eng., C* **1995**, *3*, 109; b) P. C. LeBaron, Z. Wang, T. J. Pinnavaia, *Appl. Clay Sci.* **1999**, *15*, 11; c) N. Abacha, M. Kubouchi, T. Sakai, *eXPRESS Polym. Lett.* **2009**, *3*, 245.

[8] M. Selvakumar, G. B. Nando, S. Chattopadhyay, *Advances in Polymer Materials and Technology*, CRC Press, Boca Raton, FL **2016**, p. 79.

[9] a) J. Xiong, Z. Zheng, H. Jiang, S. Ye, X. Wang, *Composites, Part A* **2007**, *38*, 132; b) Y. Kishimoto, F. Ito, H. Usami, E. Togawa, M. Tsukada, H. Morikawa, S. Yamanaka, *Int. J. Biol. Macromol.* **2013**, *57*, 124.

[10] Z. Wang, T. J. Pinnavaia, *Chem. Mater.* **1998**, *10*, 3769.

[11] G. T. Howard, *Int. Biodeterior. Biodegrad.* **2002**, *49*, 245.

[12] M. W. Moler, D. A. Kunz, T. Lunkenbein, S. Sommer, A. Nennemann, J. Breu, *Adv. Mater.* **2012**, *24*, 2142.

[13] S. Jayrajsinh, G. Shankar, Y. K. Agrawal, L. Bakre, *J. Drug Delivery Sci. Technol.* **2017**, *39*, 200.

[14] S. S. Ray, M. Okamoto, *Prog. Polym. Sci.* **2003**, *28*, 1539.

[15] M. Okamoto, S. Morita, Y. H. Kim, T. Kotaka, H. Tateyama, *Polymer* **2001**, *42*, 1201.

[16] A. Barick, D. Tripathy, *J. Appl. Polym. Sci.* **2010**, *117*, 639.

[17] A. K. Barick, D. K. Tripathy, *Appl. Clay Sci.* **2011**, *52*, 312.

[18] a) T.-K. Chen, Y.-I. Tien, K.-H. Wei, *Polymer* **2000**, *41*, 1345; b) Y. Chen-Yang, H. Yang, G. Li, Y. Li, *J. Polym. Res.* **2005**, *11*, 275.

[19] M. Mousa, N. D. Evans, R. O. C. Oreffo, J. I. Dawson, *Biomaterials* **2018**, *159*, 204.

[20] A. K. Gaharwar, L. M. Cross, C. W. Peak, K. Gold, J. K. Carrow, A. Brokesh, K. A. Singh, *Adv. Mater.* **2019**, *31*, 1900332.

[21] M. X. Liu, R. Fakhrullin, A. Novikov, A. Panchal, Y. Lvov, *Macromol. Biosci.* **2019**, *19*, 1800419.

[22] D. Chimene, R. Kaunas, A. K. Gaharwar, *Adv. Mater.* **2019**, *32*, 1902026.

[23] Y. Zhou, A. M. LaChance, A. T. Smith, H. F. Cheng, Q. F. Liu, L. Y. Sun, *Adv. Funct. Mater.* **2019**, *29*, 1807611.

[24] R. F. Giese, C. J. Van Oss, *Colloid and Surface Properties of Clays and Related Minerals*, CRC Press, Boca Raton, FL **2002**.

[25] J. J. Shao, K. Raidongia, A. R. Koltonow, J. X. Huang, *Nat. Commun.* **2015**, *6*, 7602.

[26] S. Pavlidou, C. Papaspyrides, *Prog. Polym. Sci.* **2008**, *33*, 1119.

[27] S. D. Sadhu, M. Maiti, A. K. Bhowmick, *Current Topics in Elastomers Research*, CRC Press, Boca Raton, FL **2008**, p. 40.

[28] J. Lagaron, L. Cabedo, D. Cava, J. Feijoo, R. Gavara, E. Gimenez, *Food Addit. Contam.* **2005**, *22*, 994.

[29] E. Abdullayev, A. Joshi, W. B. Wei, Y. F. Zhao, Y. Lvov, *ACS Nano* **2012**, *6*, 7216.

[30] M. L. Du, B. C. Guo, D. M. Jia, *Polym. Int.* **2010**, *59*, 574.

[31] a) E. Abdullayev, Y. Lvov, *J. Nanosci. Nanotechnol.* **2011**, *11*, 10007; b) Y. M. Lvov, D. G. Shchukin, H. Mohwald, R. R. Price, *ACS Nano* **2008**, *2*, 814.

[32] M. Morits, T. Verho, J. Sorvari, V. Liljestrom, M. A. Kostiainen, A. H. Groschel, O. Ikkala, *Adv. Funct. Mater.* **2017**, *27*, 1605378.

[33] J. Karger-Kocsis, P. Shang, Z. Mohd Ishak, M. Rösch, *eXPRESS Polym. Lett.* **2007**, *1*, 60.

[34] Y. Tien, K. Wei, *Macromolecules* **2001**, *34*, 9045.

[35] E. Bilotti, H. Fischer, T. Peijs, *J. Appl. Polym. Sci.* **2008**, *107*, 1116.

[36] E. Duquesne, S. Moins, M. Alexandre, P. Dubois, *Macromol. Chem. Phys.* **2007**, *208*, 2542.

[37] P. Liu, *Appl. Clay Sci.* **2007**, *38*, 64.

[38] a) M. Mondal, P. K. Chattopadhyay, D. K. Setua, N. C. Das, S. Chattopadhyay, *Polym. Int.* **2011**, *60*, 1334; b) A. K. Mishra, P. Rajamohanan, G. B. Nando, S. Chattopadhyay, *Adv. Sci. Lett.* **2011**, *4*, 65.

[39] S. Jin, P. H. Fallgren, J. M. Morris, Q. Chen, *Sci. Technol. Adv. Mater.* **2007**, *8*, 67.

[40] V. Rives, M. del Arco, C. Martin, *Appl. Clay Sci.* **2014**, *88–89*, 239.

[41] M. Kotal, S. K. Srivastava, A. K. Bhowmick, *Polym. Int.* **2010**, *59*, 2.

[42] G. Kahr, F. J. A. C. S. Madsen, *Appl. Clay Sci.* **1995**, *9*, 327.

[43] C. Ma, R. A. Eggleton, *Clays Clay Miner.* **1999**, *47*, 174.

[44] T. Takeichi, Y. Guo, *J. Appl. Polym. Sci.* **2003**, *90*, 4075.

[45] A. K. Mishra, S. Chattopadhyay, P. Rajamohanan, G. B. Nando, *Polymer* **2011**, *52*, 1071.

[46] M. Karesoia, H. Jokinen, E. Karalainen, P. Pulkkinen, M. Torkkeli, A. Soininen, J. Ruokolainen, H. Tenhu, *J. Polym. Sci., Part A: Polym. Chem.* **2009**, *47*, 3086.

[47] R. O. Makiniemi, P. Das, D. Honders, K. Grygiel, D. Cordella, C. Detrembleur, J. Y. Yuan, A. Walther, *ACS Appl. Mater. Interfaces* **2015**, *7*, 15681.

[48] C. Byrne, T. McNally, *Macromol. Rapid Commun.* **2007**, *28*, 780.

[49] M. Modesti, A. Lorenzetti, S. Besco, *Polym. Eng. Sci.* **2007**, *47*, 1351.

[50] J. U. Ha, M. Xanthos, *Polym. Compos.* **2009**, *30*, 534.

[51] X. Zhang, R. Xu, Z. Wu, C. Zhou, *Polym. Int.* **2003**, *52*, 790.

[52] E. Doblhofer, J. Schmidt, M. Riess, M. Daab, M. Suntinger, C. Habel, H. Bargel, C. Hugenschmidt, S. Rosenfeld, J. Breu, T. Scheibel, *ACS Appl. Mater. Interfaces* **2016**, *8*, 25535.

[53] a) W.-N. Kim, W.-J. Seo, J.-S. Han, *Google Patents*, **2009**; b) W. Seo, Y. Sung, S. Han, Y. Kim, O. Ryu, H. Lee, W. Kim, *J. Appl. Polym. Sci.* **2006**, *101*, 2879.

[54] M. Mondal, P. K. Chattopadhyay, S. Chattopadhyay, D. K. Setua, *Thermochim. Acta* **2010**, *510*, 185.

[55] M. Mondal, P. K. Chattopadhyay, D. Setua, N. Das, S. Chattopadhyay, *Adv. Mater. Res.* **2010**, *123–125*, 435.

[56] M. A. R. Meier, C. Barner-Kowollik, *Adv. Mater.* **2019**, *31*, 1806027.

[57] X. Jin, P. Sun, G. S. Tong, X. Y. Zhu, *Biomaterials* **2018**, *178*, 738.

[58] E. G. Kelley, J. N. L. Albert, M. O. Sullivan, T. H. Epps, *Chem. Soc. Rev.* **2013**, *42*, 7057.

[59] T. Posati, V. Benfenati, A. Sagnella, A. Pistone, M. Nocchetti, A. Donnadio, G. Ruani, R. Zamboni, M. Muccini, *Biomacromolecules* **2014**, *15*, 158.

[60] S. G. Wang, F. Y. Zheng, Y. P. Huang, Y. T. Fang, M. W. Shen, M. F. Zhu, X. Y. Shi, *ACS Appl. Mater. Interfaces* **2012**, *4*, 6393.

[61] M. Goncalves, P. Figueira, D. Maciel, J. Rodrigues, X. Y. Shi, H. Tomas, Y. L. Li, *Macromol. Biosci.* **2014**, *14*, 110.

[62] S. Basu, S. Pacelli, Y. Feng, Q. H. Lu, J. X. Wang, A. Paul, *ACS Nano* **2018**, *12*, 9866.

[63] C. W. Peak, J. Stein, K. A. Gold, A. K. Gaharwar, *Langmuir* **2018**, *34*, 917.

[64] D. Chimene, C. W. Peak, J. L. Gentry, J. K. Carrow, L. M. Cross, E. Mondragon, G. B. Cardoso, R. Kaunas, A. K. Gaharwar, *ACS Appl. Mater. Interfaces* **2018**, *10*, 9957.

[65] Y. F. Jin, W. X. Chai, Y. Huang, *ACS Appl. Mater. Interfaces* **2018**, *10*, 28361.

[66] V. P. Singh, G. S. Kapur, Shashikant, V. C, *RSC Adv.* **2016**, *6*, 59762.

[67] R. L. Qi, R. Guo, M. W. Shen, X. Y. Cao, L. Q. Zhang, J. J. Xu, J. Y. Yu, X. Y. Shi, *J. Mater. Chem.* **2010**, *20*, 10622.

[68] D. W. Howell, C. W. Peak, K. J. Bayless, A. K. Gaharwar, *Adv. Biosyst.* **2018**, *2*, 1800092.

[69] J. H. Y. Chung, A. Simmons, Q. H. Zeng, L. A. Poole-Warren, *Eur. Polym. J.* **2013**, *49*, 652.

[70] N. K. Singh, B. P. Das Purkayastha, J. K. Roy, R. M. Banik, P. Gonugunta, M. Misra, P. Maiti, *J. Mater. Chem.* **2011**, *21*, 15919.

[71] A. W. Ajmal, F. Masood, T. Yasin, *Appl. Clay Sci.* **2018**, *156*, 11.

[72] Y. Andriani, I. C. Morrow, E. Taran, G. A. Edwards, T. L. Schiller, A. F. Osman, D. J. Martin, *Acta Biomater.* **2013**, *9*, 8308.

[73] A. Wang, A. J. Hsieh, G. C. Rutledge, *Polymer* **2005**, *46*, 3407.

[74] a) R. Qi, R. Guo, F. Zheng, H. Liu, J. Yu, X. Shi, *Colloids Surf., B* **2013**, *110*, 148; b) Z. Wang, Y. L. Zhao, Y. Luo, S. G. Wang, M. W. Shen, H. Tomas, M. F. Zhu, X. Y. Shi, *RSC Adv.* **2015**, *5*, 2383.

[75] W. F. Lee, Y. C. Chen, *Eur. Polym. J.* **2006**, *42*, 1634.

[76] C. Yao, Z. Liu, C. Yang, W. Wang, X. J. Ju, R. Xie, L. Y. Chu, *ACS Appl. Mater. Interfaces* **2016**, *8*, 21721.

[77] L. Xiong, M. Zhu, X. Hu, X. Liu, Z. J. M. Tong, *Macromolecules* **2009**, *42*, 3811.

[78] A. Walther, I. Bjurhager, J. M. Malho, J. Pere, J. Ruokolainen, L. A. Berglund, O. Ikkala, *Nano Lett.* **2010**, *10*, 2742.

[79] P. Das, J. M. Malho, K. Rahimi, F. H. Schacher, B. C. Wang, D. E. Demco, A. Walther, *Nat. Commun.* **2015**, *6*, 5967.

[80] I. Echeverria, P. Eisenberg, A. N. Mauri, *J. Membr. Sci.* **2014**, *449*, 15.

[81] a) V. A. Kasyanov, J. Hodde, M. C. Hiles, C. Eisenberg, L. Eisenberg, L. E. F. De Castro, I. Ozolanta, M. Murovska, R. A. Draughn, G. D. Prestwich, R. R. Markwald, V. Mironov, *J. Mater. Sci.: Mater. Med.* **2009**, *20*, 329; b) K. Saha, B. S. Butola, M. Joshi, *J. Appl. Polym. Sci.* **2014**, *131*, 40230.

[82] L. P. Yang, H. X. Zhou, G. Y. Shi, Y. Wang, C. Y. Pan, *J. Polym. Sci., Part A: Polym. Chem.* **2008**, *46*, 6641.

[83] Z. Yenice, M. A. Tasdelen, A. Oral, C. Guler, Y. Yagci, *J. Polym. Sci., Part A: Polym. Chem.* **2009**, *47*, 2190.

[84] M. A. Tasdelen, *Eur. Polym. J.* **2011**, *47*, 937.

[85] W. S. Kim, J. Yi, D. H. Lee, I. J. Kim, W. J. Son, J. W. Bae, W. Kim, *J. Appl. Polym. Sci.* **2010**, *116*, 3373.

[86] W. J. Wood, R. G. Maguire, W. H. Zhong, *Composites Part B: Engineering* **2011**, *42*, 584.

[87] Z. Y. Tang, N. A. Kotov, S. Magonov, B. Ozturk, *Nat. Mater.* **2003**, *2*, 413.

[88] J. F. Wang, Q. F. Cheng, L. Lin, L. Jiang, *ACS Nano* **2014**, *8*, 2739.

[89] G. R. da Silva, A. da Silva-Cunha, F. Behar-Cohen, E. Ayres, R. L. Orefice, *Mater. Sci. Eng., C* **2011**, *31*, 414.

[90] A. Mishra, B. P. Das Purkayastha, J. K. Roy, V. K. Aswal, P. Maiti, *J. Phys. Chem. C* **2012**, *116*, 2260.

[91] T. R. Thatiparti, S. Tammishetti, M. V. Nivasu, *J. Biomed. Mater. Res., Part B* **2010**, *92B*, 111.

[92] P. Nayak, S. K. Sahoo, A. Behera, P. K. Nanda, P. L. Nayak, B. C. Guru, *World J. Nano Sci. Eng.* **2011**, *1*, 27.

[93] M. X. Liu, Z. X. Jia, D. M. Jia, C. R. Zhou, *Prog. Polym. Sci.* **2014**, *39*, 1498.

[94] X. J. Zhang, G. Lin, R. Abou-Hussein, M. K. Hassan, I. Noda, J. E. Mark, *Eur. Polym. J.* **2007**, *43*, 3128.

[95] E. Ayres, R. L. Oréfice, D. Sousa, *Macromol. Symp.* **2006**, *245*, 330.

[96] P. Kumar, K. P. Sandeep, S. Alavi, V. D. Truong, R. E. Gorga, *J. Food Sci.* **2010**, *75*, N46.

[97] Q. Zhang, Q. F. Liu, J. E. Mark, I. Noda, *Appl. Clay Sci.* **2009**, *46*, 51.

[98] A. Silvestri, P. M. Serafini, S. Sartori, P. Ferrando, F. Boccafoschi, S. Milione, L. Conzatti, G. Ciardelli, *J. Appl. Polym. Sci.* **2011**, *122*, 3661.

[99] D. K. Jena, P. K. Sahoo, *J. Appl. Polym. Sci.* **2018**, *135*, 45968.

**ADVANCED
SCIENCE NEWS**
www.advancedsciencenews.com

**ADVANCED
FUNCTIONAL
MATERIALS**
www.afm-journal.de

[100] a) N. Fong, L. A. Poole-Warren, A. Simmons, *J. Biomed. Mater. Res., Part B* **2013**, *101B*, 310; b) N. Fong, A. Simmons, L. A. Poole-Warren, *Acta Biomater.* **2010**, *6*, 2554.

[101] H. M. Park, G. H. Kim, C. S. Ha, *Compos. Interfaces* **2007**, *14*, 427.

[102] S. Srivastava, A. Biswas, S. Senapati, B. Ray, D. Rana, V. K. Aswal, P. Maiti, *Polymer* **2017**, *110*, 95.

[103] I. Larraza, C. Peinado, C. Abrusci, F. Catalina, T. Corrales, *J. Photochem. Photobiol., A* **2011**, *224*, 46.

[104] M. C. Wang, J. J. Lin, H. J. Tseng, S. H. Hsu, *ACS Appl. Mater. Interfaces* **2012**, *4*, 338.

[105] W. M. Choi, T. W. Kim, O. O. Park, Y. K. Chang, J. W. Lee, *J. Appl. Polym. Sci.* **2003**, *90*, 525.

[106] L. A. Poole-Warren, B. Farrugia, N. Fong, E. Hume, A. Simmons, *Appl. Surf. Sci.* **2008**, *255*, 519.

[107] K. E. Styan, D. J. Martin, A. Simmons, L. A. Poole-Warren, *Acta Biomater.* **2012**, *8*, 2243.

[108] A. Mishra, B. P. Das Purkayastha, J. K. Roy, V. K. Aswal, P. Maiti, *Macromolecules* **2010**, *43*, 9928.

[109] A. J. Mieszawska, J. G. Llamas, C. A. Vaiana, M. P. Kadakia, R. R. Naik, D. L. Kaplan, *Acta Biomater.* **2011**, *7*, 3036.

[110] E. Ruiz-Hitzky, P. Aranda, M. Darder, G. Rytwo, *J. Mater. Chem.* **2010**, *20*, 9306.

[111] S. Lee, S. Cho, M. Kim, G. Jin, U. Jeong, J. H. Jang, *ACS Appl. Mater. Interfaces* **2014**, *6*, 1082.

[112] R. F. Fakhrullin, Y. M. Lvov, *Nanomedicine* **2016**, *11*, 2243.

[113] F. E. Ahmed, B. S. Lalia, R. Hashaikeh, *Desalination* **2015**, *356*, 15.

[114] J. D. Schiffman, C. L. Schauer, *Polym. Rev.* **2008**, *48*, 317.

[115] a) Y. F. Jin, C. C. Liu, W. X. Chai, A. Compaan, Y. Huang, *ACS Appl. Mater. Interfaces* **2017**, *9*, 17457; b) N. Soffer-Tsur, M. Shevach, A. Shapira, D. Peer, T. Dvir, *Biofabrication* **2014**, *6*, 035023. c) P. Kerativitayanan, M. Tatullo, M. Khariton, P. Joshi, B. Perniconi, A. K. Gaharwar, *ACS Biomater. Sci. Eng.* **2017**, *3*, 590; d) F. Samani, M. Kokabi, M. Soleimani, M. R. Valojerdi, *Polym. Int.* **2010**, *59*, 901; e) D. H. Lee, N. Tripathy, J. H. Shin, J. E. Song, J. G. Cha, K. D. Min, C. H. Park, G. Khang, *Int. J. Biol. Macromol.* **2017**, *95*, 14; f) L. S. O. Pires, M. H. F. V. Fernandes, J. M. M. de Oliveira, *Int. J. Adv. Des. Manuf. Technol.* **2018**, *98*, 2665; g) P. Gatenholm, H. Martinez, J. Sundberg, S. Samfors, S. Johannesson, D. Hagg, *Abstr. Pap., Am. Chem. Soc.* **2013**, *245*; h) C. P. Jiang, Y. Y. Chen, M. F. Hsieh, *Mater. Sci. Eng., C* **2013**, *33*, 680.

[116] C. Yang, T. Zhu, J. Wang, S. Chen, W. Li, *RSC Adv.* **2015**, *5*, 69423.

[117] S. Tohidi, A. Ghaee, J. Barzin, *Polym. Adv. Technol.* **2016**, *27*, 1020.

[118] a) N. Kotobuki, K. Murata, K. Haraguchi, *J. Biomed. Mater. Res., Part A* **2013**, *101A*, 537; b) A. Paul, V. Manoharan, D. Krafft, A. Assmann, J. A. Uquillas, S. R. Shin, A. Hasan, M. A. Hussain, A. Memic, A. K. Gaharwar, A. Khademhosseini, *J. Mater. Chem. B* **2016**, *4*, 3544.

[119] S. G. Wang, R. Castro, X. An, C. L. Song, Y. Luo, M. W. Shen, H. Tomas, M. F. Zhu, X. Y. Shi, *J. Mater. Chem.* **2012**, *22*, 23357.

[120] M. Atrian, M. Kharaziha, R. Emadi, F. Alihosseini, *Appl. Clay Sci.* **2019**, *174*, 90.

[121] R. L. Qi, R. Guo, F. Y. Zheng, H. Liu, J. Y. Yu, X. Y. Shi, *Colloids Surf., B* **2013**, *110*, 148.

[122] J. H. Hong, E. H. Jeong, H. S. Lee, D. H. Baik, S. W. Seo, J. H. Youk, *J. Polym. Sci., Part B: Polym. Phys.* **2005**, *43*, 3171.

[123] R. L. Qi, X. Y. Cao, M. W. Shen, R. Guo, J. Y. Yu, X. Y. Shi, *J. Biomater. Sci., Polym. Ed.* **2012**, *23*, 299.

[124] Z. M. O. Rzayev, M. Simsek, K. Salimi, *Polym.-Plast. Technol. Eng.* **2015**, *54*, 1723.

[125] Y. L. Zhao, S. G. Wang, Q. S. Guo, M. W. Shen, X. Y. Shi, *J. Appl. Polym. Sci.* **2013**, *127*, 4825.

[126] Q. Wang, J. L. Mynar, M. Yoshida, E. Lee, M. Lee, K. Okuro, K. Kinbara, T. Aida, *Nature* **2010**, *463*, 339.

[127] A. K. Gaharwar, N. A. Peppas, A. Khademhosseini, *Biotechnol. Bioeng.* **2014**, *111*, 441.

[128] M. Jaiswal, J. Xavier, J. Carrow, P. Desai, A. Gaharwar, *Abstr. Pap., Am. Chem. Soc.* **2015**, *249*.

[129] Q. Chen, L. Zhu, H. Chen, H. L. Yan, L. N. Huang, J. Yang, J. Zheng, *Adv. Funct. Mater.* **2015**, *25*, 1598.

[130] a) P. R. S. Reddy, K. M. Rao, K. S. V. K. Rao, Y. Shchipunov, C. S. Ha, *Macromol. Res.* **2014**, *22*, 832; b) G. Sharma, B. Thakur, M. Naushad, A. Kumar, F. J. Stadler, S. M. Alfadul, G. T. Mola, *Environ. Chem. Lett.* **2018**, *16*, 113; c) G. M. Raghavendra, T. Jayaramudu, K. Varaprasad, G. S. M. Reddy, K. M. Raju, *RSC Adv.* **2015**, *5*, 14351.

[131] M. G. Xia, W. J. Wu, F. W. Liu, P. Theato, M. F. Zhu, *Eur. Polym. J.* **2015**, *69*, 472.

[132] Y. Wang, D. J. Chen, *J. Colloid Interface Sci.* **2012**, *372*, 245.

[133] G. R. Gao, L. F. Wang, Y. Cong, Z. W. Wang, Y. Zhou, R. Wang, J. Chen, J. Fu, *ACS Omega* **2018**, *3*, 17914.

[134] T. Boyaci, N. Orakdogen, *Appl. Clay Sci.* **2016**, *121–122*, 162.

[135] M. Boruah, P. Gogoi, A. K. Manhar, M. Khannam, M. Mandal, S. K. Dolui, *RSC Adv.* **2014**, *4*, 43865.

[136] G. R. Mahdavinia, S. Ettehadi, M. Amini, M. Sabzi, *RSC Adv.* **2015**, *5*, 44516.

[137] A. Sheikhi, S. Afewerki, R. Oklu, A. K. Gaharwar, A. Khademhosseini, *Biomater. Sci.* **2018**, *6*, 2073.

[138] K. Haraguchi, K. Murata, T. Takehisa, *Macromol. Symp.* **2013**, *329*, 150.

[139] W. F. Lee, Y. C. Chen, *J. Appl. Polym. Sci.* **2004**, *94*, 692.

[140] J. Nath, A. Chowdhury, I. Ali, S. K. Dolui, *J. Appl. Polym. Sci.* **2019**, *136*, 47596.

[141] J. Nath, S. K. Dolui, *Appl Clay Sci* **2018**, *155*, 65.

[142] T. Maeda, M. Kitagawa, A. Hotta, S. Koizumi, *Polymers* **2019**, *11*, 250.

[143] Y. Tan, S. M. Xu, R. L. Wu, J. Du, J. L. Sang, J. D. Wang, *Appl. Clay Sci.* **2017**, *148*, 77.

[144] F. Topuz, M. Bartneck, Y. Pan, F. Tacke, *Biomacromolecules* **2017**, *18*, 386.

[145] D. H. Su, L. B. Jiang, X. Chen, J. Dong, Z. Z. Shao, *ACS Appl. Mater. Interfaces* **2016**, *8*, 9619.

[146] H. Cheng, K. Yue, M. Kazemzadeh-Narbat, Y. H. Liu, A. Khalilpour, B. Y. Li, Y. S. Zhang, N. Annabi, A. Khademhosseini, *ACS Appl. Mater. Interfaces* **2017**, *9*, 11428.

[147] M. Hasany, A. Thakur, N. Taebnia, F. B. Kadumudi, M. A. Shahbazi, M. K. Pierchala, S. Mohanty, G. Orive, T. L. Andresen, C. B. Foldager, S. Yaghmaei, A. Arpanaei, A. K. Gaharwar, M. Mehrali, A. Dolatshahi-Pirouz, *ACS Appl. Mater. Interfaces* **2018**, *10*, 34924.

[148] L. Han, X. Lu, K. Z. Liu, K. F. Wang, L. M. Fang, L. T. Weng, H. P. Zhang, Y. H. Tang, F. Z. Ren, C. C. Zhao, G. X. Sun, R. Liang, Z. J. Li, *ACS Nano* **2017**, *11*, 2561.

[149] Y. Liu, H. Meng, S. Konst, R. Sarmiento, R. Rajachar, B. P. Lee, *ACS Appl. Mater. Interfaces* **2014**, *6*, 16982.

[150] R. Waters, S. Pacelli, R. Maloney, I. Medhi, R. P. H. Ahmed, A. Paul, *Nanoscale* **2016**, *8*, 7371.

[151] Y. Tan, R. L. Wu, H. L. Li, W. C. Ren, J. Du, S. M. Xu, J. D. Wang, *J. Mater. Chem. B* **2015**, *3*, 4426.

[152] N. Eslahi, A. Simchi, M. Mehrjoo, M. A. Shokrgozar, S. Bonakdar, *RSC Adv.* **2016**, *6*, 62944.

[153] M. Ghadiri, W. Chrzanowski, W. H. Lee, A. Fathi, F. Dehghani, R. Rohanizadeh, *Appl. Clay Sci.* **2013**, *85*, 64.

[154] K. Haraguchi, K. Murata, T. Takehisa, *Macromolecules* **2012**, *45*, 385.

[155] A. K. Gaharwar, R. K. Avery, A. Assmann, A. Paul, G. H. McKinley, A. Khademhosseini, B. D. Olsen, *ACS Nano* **2014**, *8*, 9833.

[156] S. Sharifi, S. B. G. Blanquer, T. G. van Kooten, D. W. Grijpma, *Acta Biomater.* **2012**, *8*, 4233.

**ADVANCED
SCIENCE NEWS**

www.advancedsciencenews.com

**ADVANCED
FUNCTIONAL
MATERIALS**

www.afm-journal.de

[157] A. Zaharia, A. Sarbu, A. L. Radu, K. Jankova, A. Daugaard, S. Hvilsted, F. X. Perrin, M. Teodorescu, C. Munteanu, V. Fruth-Oprisan, *Appl. Clay Sci.* **2015**, *103*, 46.

[158] Z. X. Deng, T. L. Hu, Q. Lei, J. K. He, P. X. Ma, B. L. Guo, *ACS Appl. Mater. Interfaces* **2019**, *11*, 6796.

[159] S. Kim, C. Laschi, B. Trimmer, *Trends Biotechnol.* **2013**, *31*, 287.

[160] J. I. Dawson, R. O. C. Oreffo, *Adv. Mater.* **2013**, *25*, 4069.

[161] B. M. Holzapfel, J. C. Reichert, J. T. Schantz, U. Gbureck, L. Rackwitz, U. Noth, F. Jakob, M. Rudert, J. Groll, D. W. Hutmacher, *Adv. Drug Delivery Rev.* **2013**, *65*, 581.

[162] A. Skardal, M. Devarasetty, H.-W. Kang, I. Mead, C. Bishop, T. Shupe, S. J. Lee, J. Jackson, J. Yoo, S. Soker, *A. Attala, Acta Biomaterialia* **2015**, *25*, 24.

[163] N. E. Fedorovich, W. Schuurman, H. M. Wijnberg, H. J. Prins, P. R. van Weeren, J. Malda, J. Alblas, W. J. A. Dhert, *Tissue Eng., Part C* **2012**, *18*, 33.

[164] E. DeSimone, K. Schacht, A. Pellert, T. Scheibel, *Biofabrication* **2017**, *9*.

[165] N. A. Sears, D. R. Seshadri, P. S. Dhavalikar, E. Cosgriff-Hernandez, *Tissue Eng., Part B* **2016**, *22*, 298.

[166] A. Habib, B. Khoda, *J. Manuf. Processes* **2019**, *38*, 76.

[167] K. Schacht, T. Jungst, M. Schweinlin, A. Ewald, J. Groll, T. Scheibel, *Angew. Chem., Int. Ed.* **2015**, *54*, 2816.

[168] C. B. Highley, C. B. Rodell, J. A. Burdick, *Adv. Mater.* **2015**, *27*, 5075.

[169] P. S. Gungor-Ozkerim, I. Inci, Y. S. Zhang, A. Khademhosseini, M. R. Dokmeci, *Biomater. Sci.* **2018**, *6*, 915.

[170] M. Okamoto, P. H. Nam, P. Maiti, T. Kotaka, N. Hasegawa, A. Usuki, *Nano Lett.* **2001**, *1*, 295.

[171] H. W. Kang, S. J. Lee, I. K. Ko, C. Kengla, J. J. Yoo, A. Atala, *Nat. Biotechnol.* **2016**, *34*, 312.

[172] a) S. Ostrovidov, V. Hosseini, S. Ahadian, T. Fujie, S. P. Parthiban, M. Ramalingam, H. Bae, H. Kaji, A. Khademhosseini, *Tissue Eng., Part B* **2014**, *20*, 403; b) J. S. Choi, S. J. Lee, G. J. Christ, A. Atala, J. J. Yoo, *Biomaterials* **2008**, *29*, 2899.

[173] S. A. Wilson, L. M. Cross, C. W. Peak, A. K. Gaharwar, *ACS Appl. Mater. Interfaces* **2017**, *9*, 43449.

[174] Q. Gao, X. Niu, L. Shao, L.-Y. Zhou, Z. Lin, A. Sun, J. Fu, Z. Chen, J. Hu, Y. J. B. Liu, *Biofabrication* **2019**, *11*, 035006.

[175] A. Nadernezhad, O. S. Caliskan, F. Topuz, F. Afghah, B. Erman, B. Koc, *ACS Appl. Bio Mater* **2019**, *2*, 796.

[176] T. Ahlfeld, G. Cidonio, D. Kilian, S. Duin, A. R. Akkineni, J. I. Dawson, S. Yang, A. Lode, R. O. C. Oreffo, M. Gelinsky, *Biofabrication* **2017**, *9*, 034103.

[177] G. Cidonio, C. R. Alcala-Orozco, K. Lim, M. Glinka, I. Mutreja, Y.-H. Kim, J. I. Dawson, T. B. Woodfield, R. J. B. Oreffo, *Biofabrication* **2019**, *11*, 035027.

[178] S. M. Hong, D. Sycks, H. F. Chan, S. T. Lin, G. P. Lopez, F. Guilak, K. W. Leong, X. H. Zhao, *Adv. Mater.* **2015**, *27*, 4035.

[179] J. H. Guo, R. R. Zhang, L. N. Zhang, X. D. Cao, *ACS Macro Lett.* **2018**, *7*, 442.

[180] Y. F. Jin, A. Compaan, W. X. Chai, Y. Huang, *ACS Appl. Mater. Interfaces* **2017**, *9*, 20057.

[181] T. T. Chen, H. Bakhshi, L. Liu, J. Ji, S. Agarwal, *Adv. Funct. Mater.* **2018**, *28*, 1800514.

[182] J. L. Davila, M. A. d'Avila, *Int. J. Adv. Manuf. Technol.* **2019**, *101*, 675.

[183] J. R. Xavier, T. Thakur, P. Desai, M. K. Jaiswal, N. Sears, E. Cosgriff-Hernandez, R. Kaunas, A. K. Gaharwar, *ACS Nano* **2015**, *9*, 3109.

[184] X. Y. Zhai, C. S. Ruan, Y. F. Ma, D. L. Cheng, M. M. Wu, W. G. Liu, X. L. Zhao, H. B. Pan, W. W. J. Lu, *Adv. Sci.* **2018**, *5*, 1700550.

1908101 (28 of 28)